FACULTY OF BIOSCIENCE ENGINEERING

MODELLING THE ROLE OF LIANAS IN THE WATER CYCLE OF TROPICAL FOREST ECOSYSTEMS

Number of words: 20892

Long Nguyen Hoang
Student number: 01600714

Promotors: Prof. dr. ir. Hans Verbeeck, dr. ir. Félicien Meunier
Tutor: Manfredo di Porcia e Brugnera

Master's Dissertation submitted to Ghent University in partial fulfilment of the requirements for the degree of Master of Science in Environmental Sanitation

Academic year: 2017- 2018

UNIVERSITEIT GENT

Promoters

Prof. dr. ir. Hans Verbeeck

Dr. ir. Félicien Meunier

The author

Long Nguyen Hoang

Preface

Nature is governed by its own rules, but the existence of human beings somehow alters the natural flow, I believe. However, our knowledge on interactions between humans and environment has never been enough. The more mankind discovers, the more mysteries emerge from nature. Such mysteries urge my desire to embed in the environment field, especially in the relations between humans and ecosystems. I am deeply grateful to VLIR-UOS for funding my Master study and therefore, give me a wonderful opportunity to live here in Belgium and to extend my knowledge in the field. I am also thankful for Ghent University and the Faculty of Bioscience Engineering who host the master programme and provide excellent supports and favourable conditions for my study.

Second, I would like to express my sincerely appreciation of the guiding and supervision from Prof. Hans Verbeeck. Prof. Hans is the most kind and caring promotor that I have ever met. He has given me great chances to make my very first contributions for sciences.

Additionally, I want to show great gratitude to my co-promotor Dr. Félicien Meunier and my tutor Manfredo di Porcia e Brugnera. Thank you for your help and support, especially during the hard time of my study.

I also would like to say thank to Hannes De Deurwaerder, Dr. Damien Bonal, Dr. Isabelle Maréchaux, Prof. Louis Santiago, Dr. Mark De Guzman and Dr. Ya-Jun Chen who provided me the necessary data to complete this master thesis.

Finally and most importantly, I am truly grateful to my beautiful wife Trang Tran Ngoc, who is always there for me, sharing, caring and helping me through tough times.

Long Nguyen Hoang, June 2018.

Table of Contents

List of abbreviations

A_{area}	Area-based maximum leaf net carbon assimilation rate
AGB	Above ground biomass
DGVM	Dynamic Global Vegetation Model
ED	Ecosystem demography model
ED2	Ecosystem demography model version 2
ITCZ	Inter-Tropical Convergence Zone
$K_{l,max,x}$	Saturated xylem conductivity per unit leaf area
$K_{s,sat}$	Saturated xylem conductivity per unit sapwood area
PFT	Plant functional type
PV curve	Pressure-volume curve
SLA	Specific leaf area
VPD	Vapor pressure deficit
WD	Wood density
PAR	Photosynthesis active radiation
$P_{0,l}$	Leaf osmotic potential at full turgor
$P_{tlp,l}$	Leaf osmotic potential at turgor loss point
$P_{0,x}$	Xylem water potential at full turgor
$P_{50,x}$	Xylem water potential at which 50% of conductivity is lost
ε_x	Xylem bulk elastic modulus
Ψ_L	Leaf water potential
Ψ_{md}	Leaf water potential at midday
Ψ_{pd}	Leaf water potential at predawn

Abstract

Although lianas have been shown to play a critical role in the water cycle of tropical forest ecosystems, many processes remain largely unconfirmed such as the water competition between lianas and trees. Moreover, the recent observation of liana proliferation, which could constitute one of the most important structural changes that tropical forests experience, is still poorly understood. The application of Dynamic Global Vegetation Models, a strong tool for unravelling these processes, is being constrained due to the lack of liana implementation in those models. This master thesis contributes to the development of the first liana plant functional type for future application of Vegetation Models.

A meta-analysis was conducted to collect available data on stem hydraulic traits of lianas together with leaf photosynthetic and hydraulic traits. Statistical differences of hydraulic traits were observed between the growth forms. The correlations between hydraulic traits and structural traits of lianas were also computed and compared with similar state-of-the-art correlations established for tropical trees. The results revealed a trade-off between drought tolerance and water transport efficiency among liana community themselves. Furthermore, differences between liana and tree correlations were found indicating a distinction between these growth forms in their way of trade-off between drought tolerance and water transport efficiency.

The correlations were then used to parameterize lianas in a dynamic vegetation model (i.e. the Ecosystem Demography model, ED2). Long-term simulation of a tropical moist forest in Paracou, French Guiana, revealed a significant reduction of biomass when including the lianas in the simulations. Lianas were also shown to contribute substantially to the total forest transpiration. Furthermore, the simulation indicated that the climbers not only competed directly with tree species for water resources but also indirectly influenced the competition among tree species. On the other hand, site evaluation showed that the integration of lianas and their new hydraulic parameters improved the model performance and generated more realistic simulations, e.g. in terms of evapotranspiration, sap flow and liana water-use strategy.

1. Introduction

Tropical forests are crucial components of the Earth system. They store about half of the global forest carbon stocks (Pan, et al., 2011) and therefore substantially impact land surface feedbacks to climate change. Lianas are one of the key growth forms in tropical forest ecosystems. Liana species belong to the polyphyletic group of woody plants that climb to the top of the canopy using the architecture of other plants. This growth strategy, according to Schnitzer and Bongers (2002), allows lianas to allocate more resources to reproduction, canopy development, and stem and root elongation instead of structural support. On the other hand, the woody climbers remain rooted to the ground throughout their lives. This characteristic distinguishes them from other structural parasites (e.g. epiphytes and hemiepiphytes) (Schnitzer & Bongers, 2002). Recent observations have shown a significant increase in the abundance and biomass of lianas in South America over the past 20 years (Schnitzer & Bongers, 2011; Laurance, et al., 2014). This liana proliferation is still poorly understood but believed to have a negative impact on the carbon stocks of tropical forests (van der Heijden, et al., 2015). Nevertheless, lianas are currently, according to Verbeeck and Kearsley (2016), not being accounted in any single global vegetation model. Given the context, this lack of lianas in tropical forest modelling is striking.

The first liana plant functional type is being developed at CAVElab, Ghent University within the Ecosystem demography model (ED2) (di Porcia e Brugnera, et al., in preparation). ED2 is a global vegetation model, which has been tested and compared to data in long-term simulations (Moorcroft, et al., 2001; Medvigy, et al., 2009; Kim, et al., 2012). However, liana hydrology, one of the key processes represented in ED2, is still poorly parameterized. The woody vines have been shown to have distinctive hydraulic properties such as more efficient vascular systems than trees (Schnitzer, 2005; Chen, et al., 2015) alongside with contrasted structural characteristics such as deeper root systems. Therefore, it is essential to complement liana hydraulic properties in the model, something which has not been done yet.

The main objective of this master thesis is to refine the model representation of liana hydrology by using existing model development (for trees) and combining it with a meta-analysis on available data. To achieve the objective, a main research question was formulated as: does the liana **water-use strategy differ from the one of trees**. In ED2, the water-use strategies are currently implemented by relating hydraulic traits to core traits of stem and leaf (Xu, et al., 2016). Thus, the main research question was examined via two specific research questions: (1) whether hydraulic traits of lianas differ from trees, and (2) whether liana hydraulic traits can be related to core traits of stem and leaf (e.g. wood density and specific leaf area) and if

they can be related, whether these relations of lianas are different from those of trees. From these research questions and main objective, three specific objectives were identified:

1) Examining the differences between hydraulic traits of lianas and tree.

   Hypothesis: A meta-analysis on existing data will reveal significant differences between hydraulic traits of lianas and trees.

2) Identifying the correlations between hydraulic traits of lianas and their traits of leaf and stem and comparing the correlations with that of trees.

   Hypothesis: A meta-analysis on existing data will reveal significant correlations between those traits of lianas, and these correlations will differ from those of trees.

3) Parameterizing liana hydraulic traits by the identified correlations, and investigating the impacts on model simulation and performance.

   Hypothesis: A new set of specific hydraulic traits will reveal the significant contribution of lianas to the water cycle and improve the model performance.

2. Literature review

2.1. The role of lianas in the water cycle of tropical forest ecosystems

As stated by Schnitzer and Bongers (2002), the role of lianas in tropical forest ecosystems is manifold. First, substantial forest process dynamics including regeneration and competition are impacted by lianas. The woody vines colonize and compete with trees below ground for nutrients and water, and above ground for light. As liana colonization impacts differ according to the involved tree species, the climbers also indirectly influence the competition between trees (Schnitzer & Bongers, 2002). For instance, slow growing trees and old trees are likelier to host lianas because they offer a larger time window and hence more opportunities for the colonization (Campanello, et al., 2016). The woody vines also favour trees with branched trunks or rough bark over trees with long branch-free boles and smooth bark. Second, lianas have a dramatic influence on the carbon sequestration of tropical forest ecosystems (van der Heijden, et al., 2015). Forest biomass could be significantly reduced via the processes of lianas impeding tree growth and increasing tree mortality (Campanello, et al., 2016). By comparing liana-free tree crowns with the infested tree crowns, Ingwell et al. (2010) showed that tree mortality doubled from 21% to 42% with liana colonization during the period of 10 years. Finally, due to their high sap flow, transpiration rate and relative abundance, lianas have a considerable impact on the whole forest ecosystem transpiration (Schnitzer & Bongers, 2002). An estimation of the contribution of lianas to the forest transpiration was provided by Restom and Nepstad (2001). They studied the three most common species of lianas and trees (in total six species) of a secondary forest in eastern Amazonia. Transpiration of stems and branches were measured during the dry season in 1995 and the wet season in 1996 using sap-flow meters based on the heat balance method. In addition, soil water content, measured down to 12 meters depth using Time Domain Reflectometry sensors installed in the walls of soil shafts, and precipitation were recorded to calculate evapotranspiration. The relative transpiration of lianas was larger than trees of the same diameter, and lianas maintained their transpiration longer. In summary, the authors estimated that the lianas accounted for 9 to 12% of the entire forest ecosystem transpiration.

As a type of plant, the role of lianas in the water cycle of tropical forest ecosystems includes water uptake, transport and transpiration. Studies about lianas have shown evidences of differences between lianas and trees in these processes (Schnitzer, 2005; Chen, et al., 2015). Schnitzer (2005) believed that the woody vines have deeper roots and more efficient vascular systems for the water transport which could explain their higher tolerability to drought stress than trees. Chen et al. (2015) confirmed this theory in a research on multiple liana and tree species in

Xishuangbanna of southern Yunnan Province, Southwest China. In total 99 individuals of 15 liana species and 34 co-occurring tree species from three primary tropical forests (karst forest, tropical seasonal forest and flood plain forest) with different soil water status were studied. They measured the sap flow and analysed hydrogen stable isotope composition in the xylem tissue and soil samples during dry and wet seasons of 2012. Leaf gas exchanges and water potentials were also recorded. The results showed that under drought-stress lianas could access and take up a higher proportion of water from deep soil layers as compared to trees. In addition, the woody vines could strongly adjust their physiological characteristics to improve their net photosynthesis efficiency (captured carbon per unit of water transpired) during the dry season. According to Chen et al. (2015), these advantages explain why lianas out-compete trees and become more abundant as drought stress impacts neotropical forests, a pattern that has been observed in many independent studies (Ingwell, et al., 2010; Schnitzer & Bongers, 2011; Yorke, et al., 2013; Laurance, et al., 2014). On the other hand, a recent study on below-ground competition by De Deurwaerder et al. (2018) showed that lianas in French Guiana, South America actually maintained an active root system in shallow soil layers and relied on superficial water during the dry season. This contradicted the generally accepted deep-root hypothesis of lianas in the previous studies. The below-ground competition in French Guiana was examined via the dual stable water isotope approach. The results illustrated a clear water resource partitioning between lianas and trees. The two species avoided direct competition as trees relocated their root system activity to deeper soil layers.

In addition, lianas also influence the water cycle due to their strong impact on the water processes of trees (Campanello, et al., 2016). Figure 1 illustrates the reduction in diurnal sap flow of the main stem when three tree species were colonized by lianas versus when they were free of the climbers (dashed vs solid lines). Lianas reduced from one third to a half tree sap flow, with the most significant reduction on the evergreen tree species (subplot a).

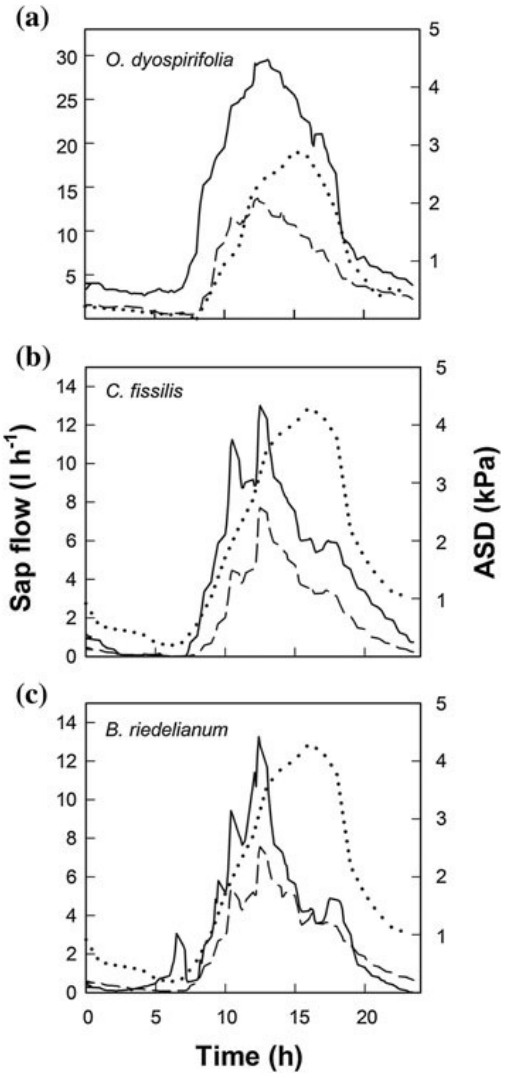

Figure 1: Diurnal sap flow at the base of main stem of three tree species that are either free (solid line) or colonized by lianas (dashed line). (a) Ocotea diospyrifolia, an evergreen species; (b) Cedrela fissilis, a deciduous species; and (c) Balfourodendron riedelianum, a brevideciduous species. The air saturation deficit (ASD) or vapor pressure deficit (VPD) is also indicated on the right axis (dotted line). Source: Campanello et al. (2016).

Overall, these studies suggest that lianas have a substantial influence on the water cycle of tropical forest ecosystems, especially in water-stressed regions. However, there are still limited studies on the link between hydraulic characteristics of lianas and their impacts on the water cycle. Moreover, the below-ground competitions for water between lianas and tree are poorly known and liana strategies for resource acquisition and utilization are largely unconfirmed.

2.2. Lianas in tropical forest ecosystem modelling

According to Castanho (2013), Dynamic Global Vegetation Models (DGVMs) can simulate average productivity and biomass close to the observations but fail to simulate spatial variability because of their weak representation of the demographic processes (Fisher, et al., 2010). Therefore, DGVMs have been unable so far to simulate realistic carbon cycles of tropical forests and one of the potential reasons is that lianas were not integrated in those model (Verbeeck & Kearsley, 2016).

Verbeeck and Kearsley (2016) argued that lianas could play a major role in addressing this problem. Indeed, lianas, as illustrated in the previous section, have substantial impacts on the biomass, transpiration and demographic processes of tropical forests. Van der Heijden (2015) showed that these woody vines strongly decrease carbon accumulation in tropical forests after conducting a large-scale liana removal experiment in a 60 years old secondary forest in Panama. Lianas were cut at the base in eight plots while no such treatment was applied to other eight control plots. Above-ground biomass was calculated by collecting litter monthly and recording diameters of trees and lianas biannually for three years. Around 76 percent of net above-ground carbon uptake was found to be lost every year due to the liana presence when the authors compared the control and the removal plots. The lost biomass was attributed to lianas impeding tree recruitment and growth, and lianas increasing tree mortality. Despite their importance, there is currently, surprisingly, no single global vegetation model accounting for the woody vines (Verbeeck & Kearsley, 2016). In the context of increasing lianas abundance in neotropical forests, the role of the woody vines in tropical forest ecosystem modelling is becoming even more vital.

The first liana PFT is being developed at CAVElab, Ghent University in the frame work of the ERC Treeclimbers project. The project objective is to implement lianas in ED2 and model them as key drivers of tropical forest responses to climate change. This master thesis contributes to project by refining liana hydrology, which is still poorly represented in the model. Currently, the hydrology of lianas is simulated using existing development for trees, though the climbers, as demonstrated above, have distinctive hydraulic properties. Therefore, it is essential to complement these distinctive properties in the model, something which has not been done yet.

2.3. The Ecosystem demography model

2.3.1 Model origin and description

Moorcroft et al. (2001) introduced a cohort-based model named the Ecosystem Demography model (ED) with a new scaling method that enabled the model to simulate realistic carbon fluxes and vegetation dynamics at regional level while being able to account for fine scale processes of tropical forests. This new scaling method consisted in a size-structured simulation that incorporated size-related heterogeneities in light available within the canopy. In addition, Moorcroft et al. (2001) for the first time kept tracking of age *a* – time since the last disturbance events (e.g. fire or death of large tree) that affected resource availability. Overall, ED consisted in a size-structured model for the ensemble mean condition of age *a*, and therefore it incorporated both the vertical size-related heterogeneities and the horizontal spatial heterogeneities. Medvigy et al. (2009) upgraded ED to ED2 by integrating the nonlinear relations between short-term and long-term processes. To do so, new biophysical components for simulating short-term fluxes of carbon, water and energy were included in ED2.

The land surface in ED2 is first divided into grid cells whose size varies from around 100 km to 0.1 km when running regional or local simulations, respectively (Medvigy, et al., 2009). These cells are different in climatology and soil properties, and are forced by gridded data sets of near-surface conditions or a coupled prognostic atmospheric model. The abiotic heterogeneity is only incorporated between the grid cells but not at sub-grid scale (Moorcroft, et al., 2001). At this finer scale, the cells consist in dynamic horizontal tiles (Figure 2a) that represent the locations with the same disturbance history, and contain dynamic vertical canopy structure. The area of the tiles depends on the proportion of canopy-gap sized area where similar canopy structure is derived from the common disturbances (Medvigy, et al., 2009). Third, within the gaps denoted as *y* (Figure 2b), individual plants occur with size *z*, however their horizontal positions are not specified. The size of a gap is approximately the size of a single canopy tree crown area. Between the gaps, only seeds are exchanged but not water or nutrients. There are also no cross-gap shading or any other sort of communications (Moorcroft, et al., 2001). The processes inside a gap include mortality with rate μ, recruitment with rate *f*, and growth of stem structure and living tissues with rate g_s and g_a, respectively. These rates are varied with plant type *x*, size *z* and resource environment *r* (Medvigy, et al., 2009). Sub-models of hydrology, decomposition and disturbance are used to simulate disturbance rate λ_F, dynamic of water *W*, carbon *C* and nitrogen *N*. Finally, at individual level (Figure 2c), the living tissue biomass B_a is distributed among leaves B_l, sapwood B_{sw} and root B_r, while the biomass of stem B_s is dead structure. Net carbon uptake

A_n and evapotranspiration Ψ are simulated hourly by a sub-model as a function of light availability, temperature, and humidity. Water *W* and nitrogen *N* taken by plant from the soil are limiting factors of net carbon uptake and evapotranspiration (Moorcroft, et al., 2001).

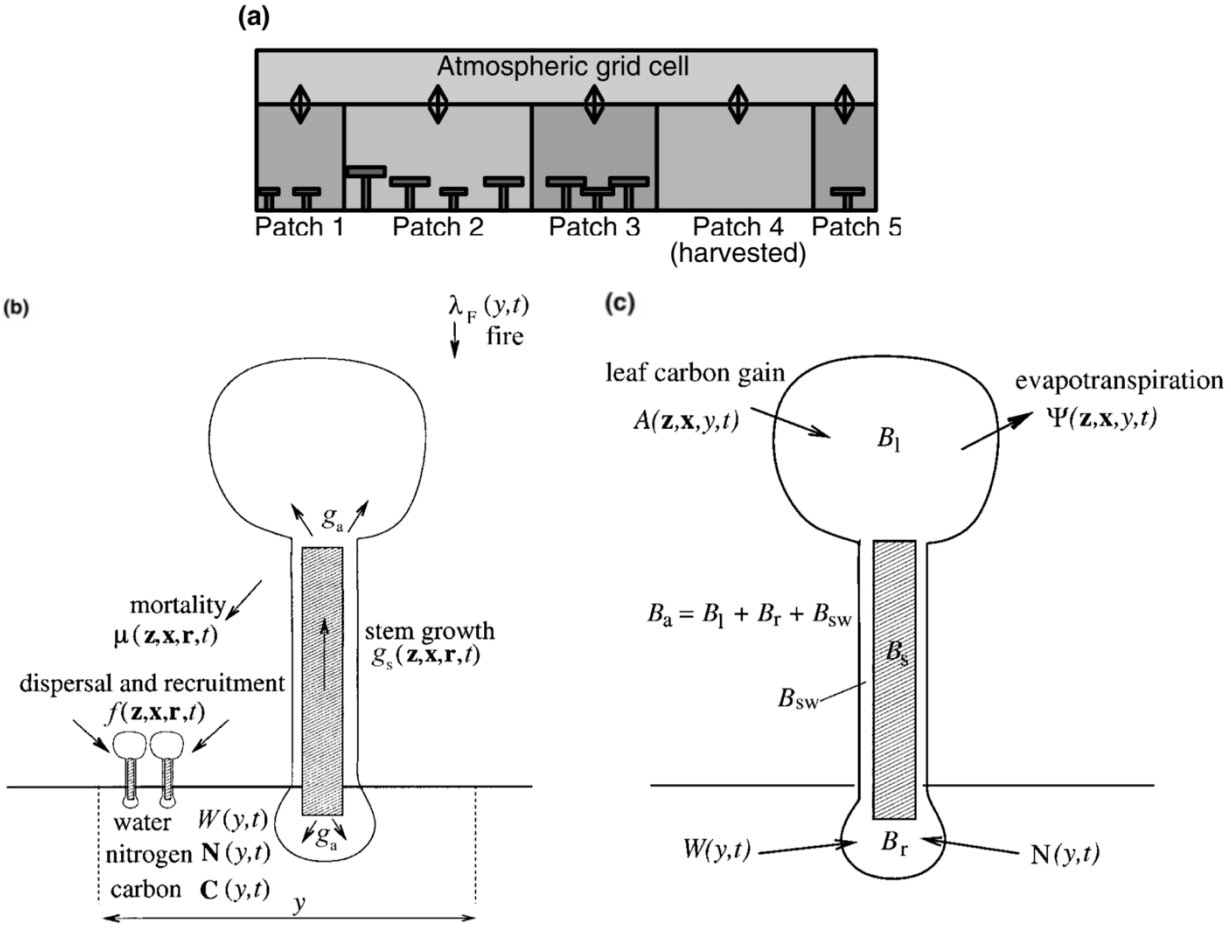

Figure 2: ED model structure and simulated processes. (a) Grid cell and tile levels (Medvigy, et al., 2009). (b) Processes within each gap and (c) at individual-level (Moorcroft, et al., 2001).

In ED2, the plant diversity is aggregated into plant functional types (PFTs). These PFTs are defined using the empirical approach of Reich et al. (1997). Different plant species are classified into a few discrete PFTs along the continuum of succession strategy using the key traits correlating among each other (Figure 3). The basic of this approach has been developed into the widely known plant economics spectrum in which different species could be arranged based on their strategies of resources utilization varying from acquisitive and fast-growing to conservative and slow-growing species (Westoby, et al., 2002; Wright, et al., 2004; Reich, 2014; Medlyn, et al., 2016).

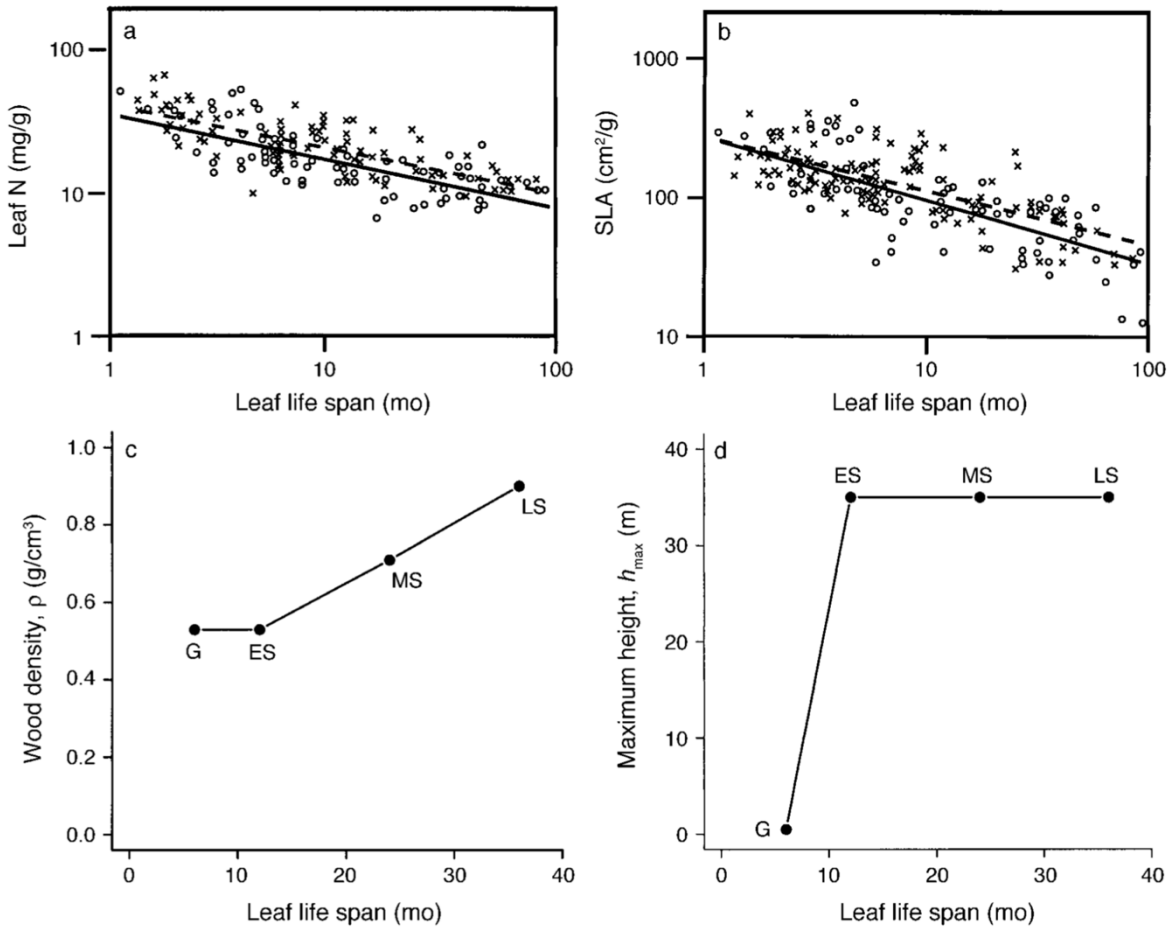

Figure 3: Continuum of plant traits used to describe the properties of the PFTs. Subplots (a) and (b) illustrate correlated changes in leaf physiological characteristics: (a) leaf nitrogen content or (b) specific leaf area as a function of the leaf longevity (Reich, et al., 1997). Graphs (c) and (d) illustrate variation in plant structural characteristic to determine the PFTs including C_4 grasses (G), early (ES), mid (MS) and late (LS) successional tree types. The relationship between leaf life span and (c) wood density or (d) maximum height are shown. Source: Moorcroft et al. (2001).

ED2 includes four main PFTs based on their relations between the traits. Along the axis in each graph (Figure 3) from left to right, the species change from grass to early (i.e. shrubs and pioneers), mid (i.e. broadleaf deciduous) and late (i.e. evergreens) successional tree types (Moorcroft, et al., 2001). For instance, the pioneer species have low wood density (WD) and high specific leaf area (SLA), and therefore they could acquire resources rapidly, grow fast and achieve early succession. In contrast, the late successional trees have higher WD and lower SLA resulting in slow resource acquisition and growth rate.

2.3.2 Recent model development for the hydrology of trees

The most recent version of ED2 is featured with three main options for the hydraulic scheme (Xu, et al., 2016). In the first scheme, plant hydrodynamics are not tracked which means the leaf and wood are always water-saturated. The second and the third scheme are featured with a plant hydraulic module that links to the existing modules of phenology, photosynthesis and soil hydraulics (Figure 4). The module simulates water flow in the soil-plant-atmosphere continuum and calculates water potential within the system of leaf and stem with a 10 minutes time step. The amount of water taken up by plant roots from different soil layers is controlled by the water potential distribution in soil and root, and the root biomass. Based on Darcy's law, the water flow from roots to the canopy is then calculated from the water potential gradient along stem and canopy, plant height, and sapwood conductance. The sapwood conductance is controlled by xylem cavitation effects. When the water potential of stem declines, xylem conductivity decreases due to embolism and the other way around with potential full recovery. Upon the canopy, transpiration depends on environmental conditions, leaf area and stomatal conductance. The stomatal conductance is calculated using an optimization-based approach (Katul, et al., 2010; Vico, et al., 2013) in which the Lagrangian multiplier technique is introduced to assess the net increase in photosynthetic gain per unit of water loss and makes the system evolve towards optimality. Finally, the water potential of leaves and stem are determined by the different water flow rates and the capacitances of the system parts. Overall, the hydraulic module in the second and third hydraulic scheme plays a major role in controlling the phenology and photosynthesis (Figure 4).

In addition to the hydraulic module, a new leaf-shedding routine in response to water stress is incorporated in the phenology module (Medlyn, et al., 2016). The previous shedding routine that occurred when soil water content declined under a critical threshold (Moorcroft, et al., 2001) failed in representing the key differences among species (Xu, et al., 2016). The new leaf-shedding routine is now based on the concept that leaf cells need to maintain their turgor for biological activity (Lockhart, 1965; Hsiao, 1973). Therefore, the shedding will occur if the predawn water potential of leaves is below the leaf osmotic potential at turgor loss point ($P_{tlp,l}$) for 10 consecutive days. In contrast, if the predawn water potential of leaves increases above half of $P_{tlp,l}$ for 10 consecutive days, leaves will regrow (Xu, et al., 2016).

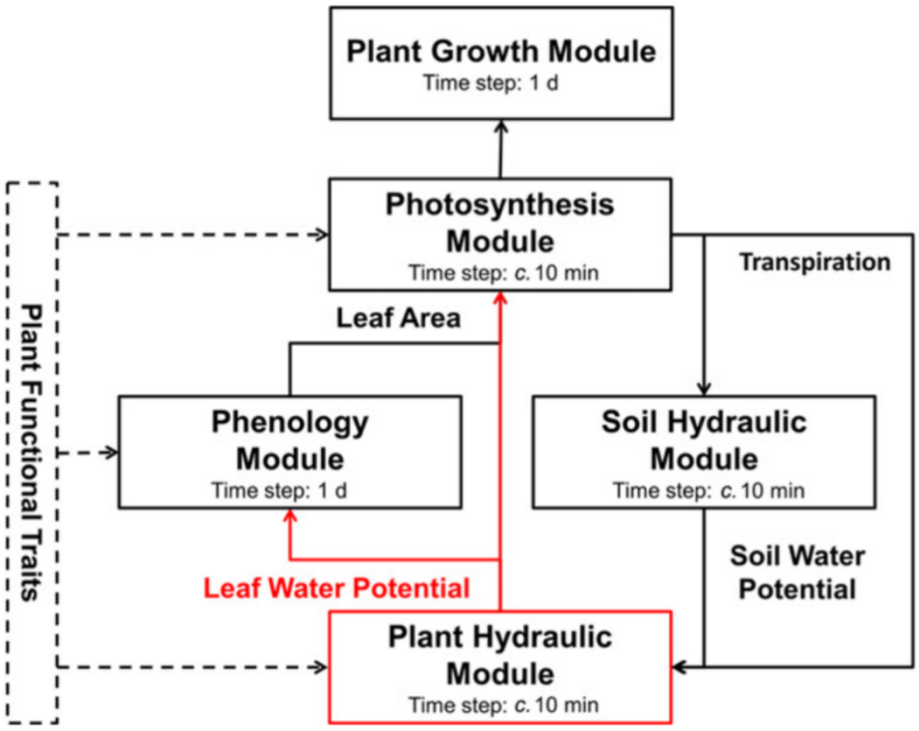

Figure 4: New framework of the updated version of ED2 developed by Xu et al. (2016)

Important parameters of the second and the third hydraulic scheme include $P_{tlp,l}$ in phenology module, area-based maximum leaf net carbon assimilation rate (A_{area}) in the photosynthesis module and saturated xylem conductivity per unit sapwood area ($K_{s,sat}$) and xylem water potential at which 50% of conductivity is lost ($P_{50,x}$) in the plant hydraulic module. $P_{tlp,l}$, which is a general term expressing the leaf water potential at which the leaf loses its turgor, is a key trait affecting plant vulnerability to drought (Maréchaux, et al., 2017). The reason is that plants depend significantly on water for their structure and support due to the large proportion of water in the biomass of non-woody tissues and due to the absence of a skeleton system. Plant cells normally exert a pressure against the cell walls which is known as turgor - the basic support mechanism for plant structure. When plants lose turgor as the soil water potential decreases, they lose certain physiological functions and ultimately die if the situation is prolonged (Lambers, et al., 2008). A_{area} is a photosynthetic trait that determines the photosynthetic efficiency of plant leaves and therefore it affects the net photosynthetic gain per unit of water loss (Xu, et al., 2016). For instance, plant with high A_{area} could utilize water more efficiently because it can assimilate more carbon per unit of water loss. $K_{s,sat}$ is the quotient of mass flow rate and pressure gradient under no effect of embolism (Sperry, et al., 1988). It determines the efficiency of water transport by plant

stem. $P_{50,x}$ is a general term widely used to compare stem vulnerability to drought-induced cavitation among species and aridity gradients (Meinzer, et al., 2009).

These traits were parameterized by a trait-based approach which was based on the plant economics spectrum. It coupled the hydraulic, phenology and photosynthesis parameters with the plant functional traits that are WD and SLA (figure 4). The second hydraulic scheme was parameterized by Xu et al. (2016) via a meta-analysis. Data of the four key parameters and their relationship with WD and SLA in seasonally dry tropical forests was collected via ISI Web of Knowledge using relevant key words. Thanks to this meta-analysis, they determined the correlations between the parameters and the two core economic traits (Figure 5). The resulted correlations of Xu et al. (2016) showed more evidences on that hydraulics traits form part of the plant economic spectrum (Medlyn, et al., 2016). For example, fast-growing species with lower WD and higher SLA tend to have a risky strategy which maximizes water uptake and use with high $K_{s,sat}$ and A_{area}. However, their relatively high $P_{tlp,l}$ and $P_{50,x}$ make them vulnerable to drought stress. In contrast, slow-growing species with higher WD and lower SLA use a conservative strategy with low $K_{s,sat}$ and A_{area}. However, they can tolerate drought stress.

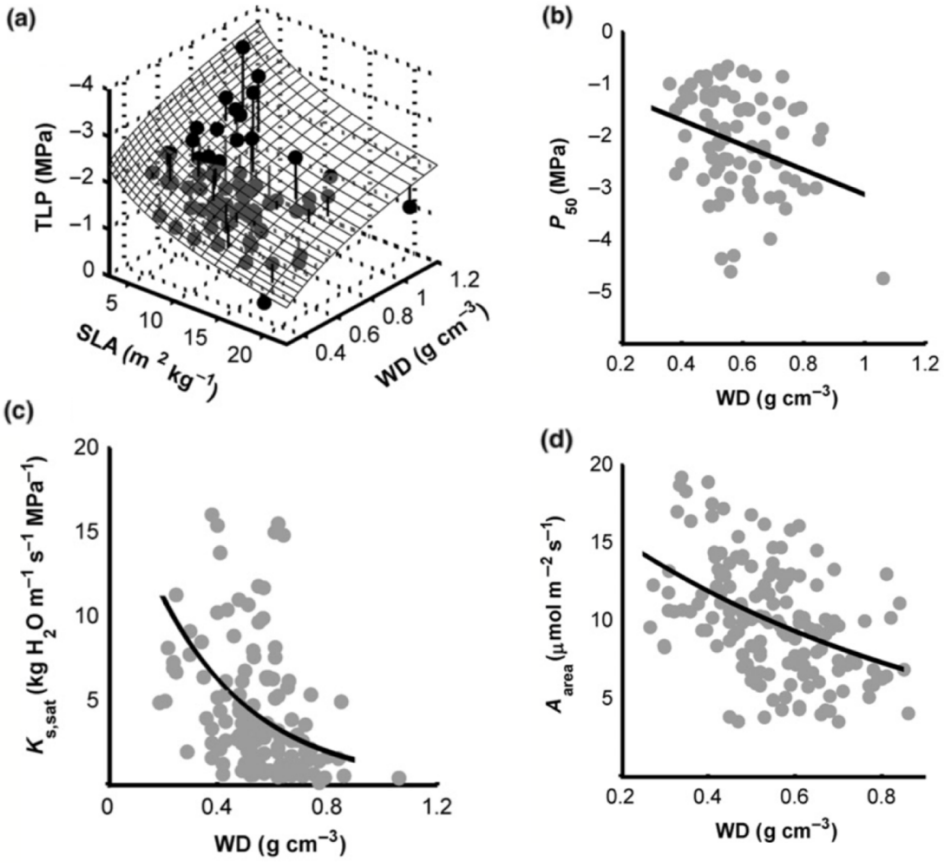

Figure 5: Relationships between hydraulic and two plant functional traits: $P_{tlp,l}$ (denoted as TLP on

graph (a) as a function of the WD and the SLA, and $P_{50,x}$ (denoted as P_{50} on graph b), $K_{s,sat}$ (graph c), and A_{area} (graph d) as a function of the WD only. Source: Xu et al. (2016)

The third hydraulic scheme was parameterized following Christoffersen et. al. (2016). The correlations between hydraulic traits and traits of leaf and stem were also constructed via synthesizing the literature and existing trait database. The collected data was open to all kind of tropical forests, and also include hydraulic traits associated with the pressure-volume curve (PV curve) which describes the relationship between water content and water potential in plant xylem. The correlations were then validated via model experiments in a seasonal evergreen forest from Caxiuana National Forest of east-central Brazilian Amazonia. This was different from the second hydraulic scheme since the meta-data analysis of Xu et. al. (2016) was limited to seasonally dry tropical forests. Moreover, $P_{tlp,l}$ was not parameterized via direct correlation with the traits of leaf and sapwood. Christoffersen et. al. (2016) calculated $P_{tlp,l}$ based on two hydraulic traits associated to PV curve which were leaf osmotic potential at full turgor ($P_{0,l}$) and xylem bulk elastic modulus (ε_x) as follows:

$$P_{tlp,l} = \frac{\varepsilon_x P_{0,l}}{\varepsilon_x + P_{0,l}}$$

Since ε_x was about 5 to 20 times larger than the absolute value of $P_{0,l}$ (Christoffersen, et al., 2016), $P_{tlp,l}$ can be approximated as follows:

$$P_{tlp,l} \approx \frac{\varepsilon_x P_{0,l}}{\varepsilon_x} = \ P_{0,l}$$

Therefore, $P_{tlp,l}$ was also negatively correlated to WD since $P_{0,l}$ decreased with an increase in WD as shown by the authors (Figure 6a). $K_{s,sat}$ was estimated via dividing saturated xylem conductivity per unit leaf area ($K_{l,max,x}$) by the ratio of leaf to sapwood, though $K_{s,sat}$ was shown to negatively correlate with WD (Figure 6c). On the other hand, $K_{l,max,x}$ and $P_{50,x}$ were directly linked to WD and they were also decreasing with an increase in WD (Figure 6d and 6b). Overall, WD drove most of the variation in the coordination among hydraulic parameters (Christoffersen, et al., 2016) and therefore, the two-hydraulic schemes to a certain extent both agreed on the correlations between hydraulic traits and the stem trait. On the other hand, A_{area} was not linked to WD in the third scheme since no significant correlation was found between them (Christoffersen, et al., 2016).

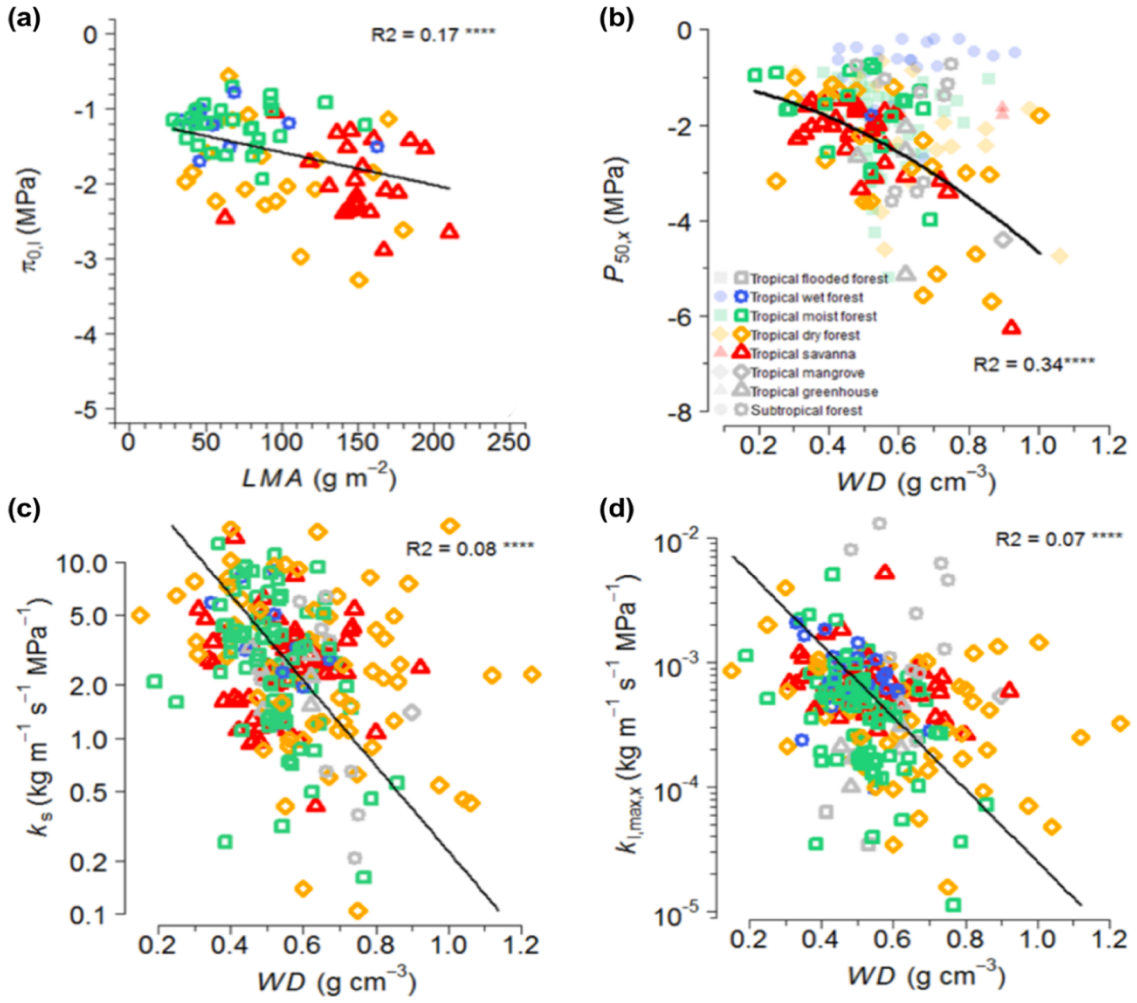

Figure 6: Relationship between four hydraulic traits ($P_{0,l}$, graph a; $P_{50,x}$, graph b; $K_{s,sat}$, graph c; $K_{l,max,x}$, graph d) and the stem trait (WD) of tree species from tropical forests. Source: Christoffersen et al. (2016).

2.4. Linking key hydraulic traits of lianas to the core economic traits

2.4.1 Key hydraulic traits of lianas

a) Saturated xylem conductivity per unit sapwood area

Zhu and Cao (2009) revealed that the average $K_{s,sat}$ of lianas was about two times higher than that of trees. Their study was conducted on three liana species and three tree species which are the most important components of the local seasonal tropical forest in southern Yunnan, China. Terminal branches with similar diameters from five individuals per species were sampled during the wet season. $K_{s,sat}$ was obtained by measuring hydraulic conductivity and embolism in xylem of Sperry et al. (1988). The branch segment was cut underwater and was then repeatedly flushed at

high pressure (about 0.1 MPa) for around 20 minutes to remove embolisms. Afterward, the maximum stem conductivity was determined by measuring the water flux (kg/s) through the stem segment and dividing the flux by the pressure gradient (MPa/m). The conductivity was further normalized by the sapwood area (m^2) to get the $K_{s,sat}$ (kg m^{-1} s^{-1} MPa^{-1}). Zhu and Cao (2009) attributed the considerable high $K_{s,sat}$ of lianas to their wider and larger vessels shown in an earlier study (Ewers, et al., 1990). These vessels helped them transport water more efficiently despite having a narrow stem. The finding of Zhu and Cao was consistent with the findings of previous studies (Ewers & Fisher, 1991; Chiu & Ewers, 1992; Field & Balun, 2008). The authors also argued that the efficiency of water transport in trees is limited by mechanical constraints of the stem (McCulloh & Sperry, 2005) that do not apply for lianas due to their dependence on the host trees for mechanical support (Zhu & Cao, 2009).

Similar results were also found in later studies with the same method but on other liana and tree species (De Guzman, et al., 2016; Chen, et al., 2017). De Guzman et al. (2016) found a mean $K_{s,sat}$ for the woody vines about twice the mean $K_{s,sat}$ of trees. Samples of six tree species and six liana species were taken during the early and mid-wet season in a seasonally dry semi-deciduous tropical forest in Parque Natural Metropolitano, Panama. The higher mean $K_{s,sat}$ of the woody vines was also shown by Chen et al. (2017) in his study on four liana species and five tree species during the wet season at the same site with Zhu and Cao.

b) Xylem water potential at which 50 percent conductivity is lost

De Guzman et al. (2016) also derived $P_{50,x}$ of lianas and trees from the hydraulic vulnerability curves that illustrate the relationship between xylem pressure and loss of conductivity (Meinzer, et al., 2009). By analysing the correlation between $P_{50,x}$ and $K_{s,sat}$ afterwards, De Guzman et al. (2016) showed evidence of a trade-off between water transport efficiency and drought tolerance in lianas and trees. The woody vines use a risky strategy with high water transport efficiency expressed in high mean $K_{s,sat}$, but are more vulnerable to drought expressed in high mean $P_{50,x}$. In contrast, trees use a conservative strategy with less water transport efficiency expressed in low mean $K_{s,sat}$ but are less vulnerable to drought expressed in low mean $P_{50,x}$. By also conducting the vulnerability curves for lianas and trees, Chen et al. (2017) supported the trade-off between water transport efficiency and drought tolerance in woody vines. More consistent results from other species can be found in an earlier study on eight liana species and thirteen tree species during the dry season in a semi-deciduous seasonally moist forest in Parque Nacional Soberania, Panama (van der Sande, et al., 2013), and in the study of Zhu and Cao (2009).

However, this trade-off of lianas, which results in being more vulnerable to drought-induced cavitation, is actually their water-use strategy for dealing with water deficits (Chen, et al., 2017). Chen et al. (2017) showed that although lianas lost almost half of the conductivity during midday, they still could transport water efficiently due to their substantially high mean $K_{s,sat}$. Furthermore, the woody vines utilized their strong physiological regulation and efficient water transport to maintain stem water potential within the safe range (above $P_{tlp,l}$) to avoid xylem dysfunction due to water deficits.

c) Leaf osmotic potential at turgor loss point

Plant species with low $P_{50,x}$ also have low $P_{tlp,l}$ (Reich, 2014). This suggests that lianas should have a mean $P_{tlp,l}$ higher than that of trees. However, this was not always the case in several studies. Zhu and Cao (2009) showed that mean $P_{tlp,l}$ of lianas was only higher than that of trees during the dry season, but the mean was actually lower than that of trees during the wet season. In the study, they measured leaf water potential with the pressure chamber and conducted the PV curves via bench drying technique. $P_{tlp,l}$ was then derived from the relationship between leaf water potential and relative water content. By also conducting the leaf PV curves at the same study site in China, Chen et al. (2017), found that the mean $P_{tlp,l}$ during the wet season was comparable among lianas and trees. In French Guiana, Maréchaux et al. (2017) showed that lianas, however, only had mean $P_{tlp,l}$ higher than that of trees during the wet season. During the dry seasons, the mean $P_{tlp,l}$ between lianas and trees was not significantly different. Her study was conducted on numerous individuals of lianas and trees sampled in 2012, 2014 and 2015. $P_{tlp,l}$ was derived in a different way with the above studies of Chen et al. (2017) and Zhu and Cao (2009). First, osmotic potential at fully hydrated leaves was measured using a vapour pressure osmometer. Afterward, a physical calibration validated at the site was used to convert the osmotic potential into $P_{tlp,l}$.

d) Area-based maximum leaf net carbon assimilation rate

Zhu and Cao (2009) used a photosynthetic system (Li-6400, LiCor, Lincoln, Nebraska, USA) to measure A_{area} from fully-expanded, healthy sun leaves of lianas and trees on consecutive sunny days during the wet season. They showed that lianas had an average A_{area} around 1.5 times higher than that of trees which indicated that lianas utilized water more efficiently. Therefore, the authors argued that lianas have an advantage over trees on photosynthesis and growth due to their relatively cheap but efficient xylem and more efficient leaves.

However, Cai et al. (2009) found no significant difference in mean A_{area} between the other species of lianas and trees during the wet season. Their study was conducted on 18 liana species and 16 tree species during wet and dry seasons in a tropical seasonal forest in Xishuangbanna, Southwest China. A_{area} was measured under a light saturating irradiance (provided by an internal red/blue LED light source) with a similar portable photosynthetic system to Zhu and Cao (2009). Mean A_{area} of lianas was found to be significantly higher than that of trees only during the dry seasons as the soil water decreased. The reason was that while lianas could maintain their relative high A_{area}, mean A_{area} of trees reduced about 60% compared to the one of the wet season. Cai et al. (2009) believed that lianas can assimilate more carbon and be more tolerable to water deficits during the dry season. By measuring A_{area} with the same photosynthetic system, Chen et al. (2015) found the consistent results at three primary tropical forests with different soil water status in Xishuangbanna. Lianas had mean A_{area} substantially higher than that of trees at the sites where there were significantly soil water deficits during the dry season. As mentioned above, this large water use efficiency could be one of the major advantages that helps lianas to out-compete trees under drought stress.

2.4.2 Linking the hydraulic traits to wood density

Lianas are expected to have low WD because of the abundance of large vessels in their tissues (Ewers & Fisher, 1991). Therefore, according to the correlations between WD and the hydraulic traits described above, the woody vines should be associated with a riskier strategy compared to trees. On one hand, they should maximize water uptake and use with $K_{s,sat}$ and A_{area} higher than those of trees. On the other hand, they should have $P_{tlp,l}$ and $P_{50,x}$ higher than those of trees which make them more vulnerable to drought stress. Indeed, lianas have been shown to have $K_{s,sat}$, A_{area} and $P_{50,x}$ higher than those of tree, though the $P_{tlp,l}$ of lianas has not been always higher than that of tree.

Nevertheless, there are evidences that lianas actually have comparable WD to trees. For instance, van der Sande (2013) showed that mean WD between 11 liana species and 13 tree species in Panama was not significantly different. Also, in Panama, a latter study on other species including 6 liana species and 6 tree species revealed that mean WD of lianas was even higher than that of trees (De Guzman, et al., 2016). De Guzman et al. (2016) believed that the WD of lianas is not determined by the large vessels. They attributed the large WD in lianas to a broad distribution of vessel sizes (Rowe & Speck, 2005) and the high vessel density resulted from the less investment in fibres needed for mechanical support (Ewers, et al., 2015). These studies

suggest that the correlations between WD and the hydraulic traits of lianas differ from those of trees, though none of the studies was able to explicitly identify the correlations for lianas.

Overall, hydraulic properties of trees and their relationship with core economic traits like WD and SLA have been widely studied. Moreover, their hydrological process and water-use strategy have been well implemented in ED2 as well as other standard DGVMs. In contrast, the relationship between important hydraulic traits and core economic traits, and some of the hydraulic properties of lianas such as $P_{tlp,l}$ are poorly known. This together with the lack of lianas in DGVMs are the major reason why the hydrological process and water-use strategy of lianas remain largely unconfirmed.

3. Materials and methods

3.1. Comparing hydraulic traits of lianas and trees

The methodology for the first specific objective consisted in a meta-analysis of four key functional traits that are central to parameterize the hydraulic modules: $K_{s,sat}$, $P_{50,x}$, $P_{tlp,l}$, and A_{area}. The records of the four traits together with WD and SLA of lianas were synthesized from existing literature using the ISI Web of Knowledge search engine with keywords such as "xylem conductivity, liana", "xylem vulnerability, liana", "turgor loss point, liana" and "gas exchange, liana". The result database was complemented by the TRY database (https://www.try-db.org) and unpublished datasets from close lab collaborators. 18 records of $P_{tlp,l}$ from 18 species were found. In which, nine records were unpublished data obtained from Louis Santiago (Professor at Department of Botany & Plant Sciences, University of California, Riverside, USA), and Isabelle Maréchaux (Post-doc at Laboratoire Evolution et Diversité Biologique, Université Paul Sabatier, Toulouse, France). Three unpublished records of WD and SLA, acquired from Ya-Jun Chen (Associate Professor at Key Laboratory of Tropical Forest Ecology, University of Chinese Academy of Sciences, Beijing, China), were added to the dataset. For xylem hydraulic traits, 24 records from 23 species and 28 records from 26 species were found for $P_{50,x}$ and $K_{s,sat}$, respectively. Two unpublished records of the xylem hydraulic traits were provided by Louis Santiago and three unpublished records of WD were provided by Ya-Jun Chen. For the photosynthetic trait, 21 records of A_{area} from 18 species were collected. This dataset included seven unpublished WD records obtained from Louis Santiago and Ya-Jun Chen. Finally, the species-averaged WD was estimated using The Global WD Database (Chave, et al., 2009; Zanne, et al., 2009) and then added to the liana database where it was unreported.

For tree data, the database of Christoffersen et al. (2016) was reconstructed. Leaf PV curve dataset (e.g. $P_{tlp,l}$) was synthesized from Bartlett et al. (2012) and Bartlett et al. (2014) database subset for tropical ecosystem, Maréchaux et al. (2015) dataset, and new data synthesized in the paper of Christoffersen et al. (2016). The dataset was then complemented with species-averaged WD from The Global WD Database. Dataset of xylem functional traits and leaf photosynthetic trait (e.g. $K_{s,sat}$, $P_{50,x}$ and A_{area}) was constructed from Xylem Functional Traits Database (Choat, et al., 2012; Gleason, et al., 2016) subset for tropical ecosystem and new data synthesized in the paper of Christoffersen et al. (2016). There was limited number of A_{area} records (around 50 records) in comparison with 121, 124 and 130 records of $P_{tlp,l}$ $K_{s,sat}$ and $P_{50,x}$, respectively. Thus, the A_{area} dataset was further merged with the readily available dataset of Xu et al. (2016).

WD has been shown to be strongly correlated with the key functional traits of trees and drives most of the variation in the coordination among key parameters in the hydraulic schemes of ED2. Therefore, differences between WD ranges of liana records and tree records could substantially affect the results of the comparison. To avoid this, the WD range of liana records was used as a constraint and all tree records outside the liana WD range were not considered. t-tests were performed using R statistical packages (R Core Team, 2017) to test the differences between the key functional traits of lianas and trees. In addition, $K_{s,sat}$ was log-transformed before analysis to meet the normality requirement.

3.2. Linking hydraulic traits of lianas to core traits of stem and leaf

For the second specific objective, the meta-analysis continued to be used to investigate whether the four key functional traits could be linked to WD and SLA. Since, WD and SLA were shown to be good predictive variables of $P_{tlp,l}$ of trees (Xu, et al., 2016), a step-wise linear regression was performed to test whether both WD and SLA can also be predictive variables of $P_{tlp,l}$ of lianas. For the other traits, linear regressions were tested with WD as the only predictive variable. Except for WD in $K_{s,sat}$ dataset, log-transforms of WD, negative $P_{tlp,l}$, negative $P_{50,x}$ and $K_{s,sat}$ were performed beforehand to meet the normality requirement.

3.3. Implementing and testing new hydraulic traits of lianas

3.3.1 Study area

The study site for implementing and testing the new hydraulic traits of lianas is the Guyaflux experimental unit, French Guiana, South America. As described by Bonal et al. (2008), this study area consists of more than 400 ha undisturbed forest and the footprint of Guyaflux tower. The ecosystem here is pristine, tropical wet forest with mean tree density of 620 trees/ha (tree with diameter at breast height more than 0.1 m) and tree species richness of around 140 species/ha. In addition, the average height of tree is 35m with emergent trees exceeding 50m.

Also according to Bonal et al. (2008), the climate of study site is wet tropical climate with large seasonal variations in rainfall driven by the north/south movement of the Inter-Tropical Convergence Zone (ITCZ). There are heavy rains from December to February and from April to July when the ITCZ is above the area. Afterwards, there is a short dry period from August to November. The mean of annual precipitation from 2004 to 2016 was around 3078 mm. The two main seasons can be seen in Figure 7. In contrast with precipitation, the mean temperature is quite stable throughout the year with an annual mean of 25.7^{o}C (Figure 7). In addition, the study

site does not have strong winds with speed above 20 m/s. The wind speed is averaged 2-3 m/s with main direction of east-northeast.

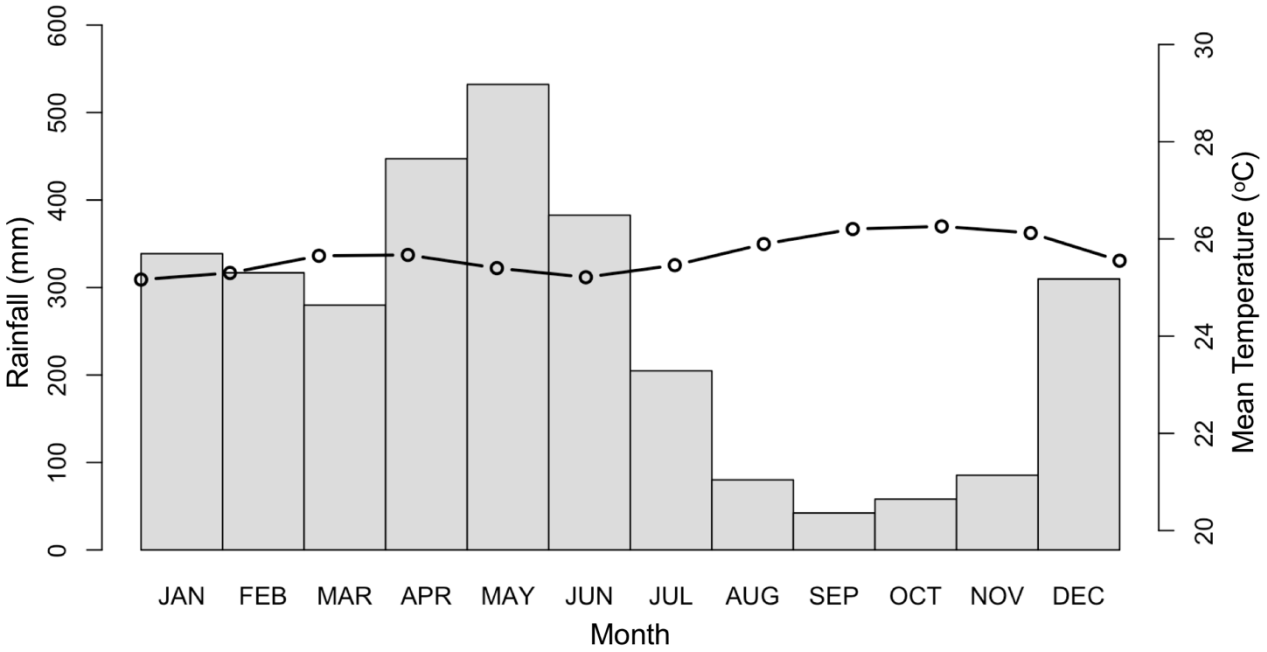

Figure 7: Monthly rainfall (bars) and mean temperature (dashed line) averaged from 2004 to 2016. Data from Guyaflux flux tower.

The study site mainly covers a relief of large hills over schist rock, a bottomland (50–100 m wide) with a small (1 m wide) creek, and a transition zone between the hills and a sandy plateau over migmatite rock (Bonal, et al., 2008). The soils in the area are mostly nutrient-poor acrisol composed of schist and sand stone (FAO-ISRIC-ISSS, 1998). According to Bonal et al. (2008), the soils are characterized by pockets of sandy utisols developed over a Precambrian metamorphic formation.

The Guyaflux tower is a 55 m high self-supporting metallic tower located in the western part of the study site. Meteorological and eddy flux sensors are installed 3 m above the tower and around 23 m above the overall canopy (Bonal, et al., 2008). From December 2003, the tower has been recording microclimate and eddy covariance data every half hour using the Euroflux methodology of Aubinet et al. (1999).

3.3.2 Model experiment

The results of meta-analysis were used to parameterize the four key functional traits of lianas and trees in ED2. The impacts of new liana traits on model simulation were then examined by two model experiments in French Guiana: a long-term simulation from bare ground and a seasonal

simulation (e.g. dry season versus wet season). The meteorological forcing data was obtained from Guyaflux tower and the soil data was from FAO-ISRIC-ISSS (1998). The PFTs in the experiments included early, mid and late successional tree PFTs and liana PFT. The hydraulic scheme used was parameterized following Christoffersen et. al. (2016). The parameters in this scheme were synthesized from data of all tropical forest kinds and were validated in a seasonal evergreen forest from South America and therefore, they were closely related to the conditions of the study site. In addition, three model setups were formulated including a control setup without liana PFT (denoted as noLian), a setup with liana PFT but parameterized in the same way as the tree PFTs (denoted as Lian) and a setup with liana PFT parameterized with the new liana parameters resulted from the meta-analysis (denoted as Lian+Param). Comparison between the results of noLian and Lian+Param allowed to determine the impacts of lianas on the carbon stocks and water cycle of French Guiana. Meanwhile, comparison between the results of Lian and Lian+Param revealed impacts of the new hydraulic traits parameterized specifically for lianas on model simulation.

The long-term simulation was initiated from bare ground with duration of 300 years. The meteorological forcing dataset spanned years from 2004 to 2012 of Guyaflux tower recycled over 300 years. The outputs of above ground biomass (AGB), leaf biomass, storage biomass and leaf water transpiration were analysed. These outputs were monthly mean of different cohorts that are collections of plants of identical PFT and height simulated by ED2. The values of cohorts with the same PFT were summed up and these PFT values from twelve months were then averaged as yearly means.

The seasonal simulation consisted of a dry month (September 2009) and a wet month (April 2010). September 2009 was chosen because it had the lowest monthly precipitation (about 0.4 mm) in the twelve years data records. In the next wet season of 2010, April had the highest precipitation (more than 700 mm). The outputs of leaf transpiration and leaf water potential (Ψ_L) were analysed. These outputs were half-hour time-step values of different cohorts. For leaf transpiration, the values of cohorts with the same PFT were summed up. Meanwhile, weighted means of Ψ_L of cohorts with the same PFT were calculated using the weighting factor of leaf area index. These PFT values for each time step from all the days in dry/wet months were then averaged to show the impacts on variation during the days of the two seasons. Moreover, the impacts on Ψ_L of lianas were further examined via the values and correlation of Ψ_L at predawn – 6:00 (Ψ_{pd}) and leaf water potential at midday – 14:00 (Ψ_{md}) during the dry month.

3.3.3 Model evaluation

The new liana parameters were evaluated via model simulation of evapotranspiration and sap flow compared with observation data in French Guiana. The sources of meteorological forcing data and soil data were similar with in model experiments. Moreover, the involving PFTs, hydraulic scheme and three model setups were also the same.

The model evaluation of evapotranspiration was first implemented by further analysing the outputs of the seasonal simulation from model experimental session. Total evapotranspiration was computed for every half-hour by adding total transpiration, and soil, leaf and wood evaporation of the whole study site. These values for each time step from all the days in dry/wet months were then averaged to show the impacts on variation during the days of the two seasons. For larger time-scale evaluation, a short-term simulation from 2005 to 2016 was conducted. The meteorological forcing dataset was data from the same period of Guyaflux tower. The observation data was latent heat flux (W/m^2 or $J/m^2/s$) obtained also from Guyaflux tower. Evapotranspiration ($kg/m^2/day$ or mm/day) was computed from the latent heat flux using equivalent evaporation of 1 mm/day equalling to 2.45 $MJ/m^2/day$ at 20°C (FAO, 1998). The simulation outputs were monthly means of total transpiration, and soil, leaf and wood evaporation of the study site. Total evapotranspiration was again derived by taking sum of these outputs. The monthly means of total evapotranspiration in 2016 were evaluated. In addition, the yearly means from 2005 to 2016 were also computed and compared to observations.

The model evaluation of sap flow was a seasonal simulation that consisted of two dry months with precipitation lower than 100 mm (November 2015 and January 2016) and two wet months with precipitation more than 500 mm (April and May 2016). These months were chosen based on the availability of observation data which was sap flow density (kg per dm^{-2} of sapwood area per hour) of one liana species and four tree species in the study site. The sap flow density was measured every half-hour by Granier-type sensors. The tree species were Sloanea sp., Goupia glabra, Oxandra asbeckii and Licania membranacea with WD acquired from The Global WD Database of 0.495, 0.727, 0.770 and 0.880 g/cm^3, respectively. The sap flow data of these tree species was used to evaluate the simulation of early, mid and late PFTs based on the similarity between WD of the species and the PFTs. The current WD values of early, mid and late PFTs in ED2 model are 0.530, 0.710 and 0.900 g/cm^3, respectively. The outputs were half-hour time-step values of sap flow (kg/h) of different cohorts. The basal area (total cross-sectional area of stems per ha soil) of each tree cohort was converted to basal sapwood area (total cross-sectional area of sapwood per ha soil) by the equation developed by Meinzer et al. (2005) for tropical trees:

$$Basal\ sapwood\ area\ \left(\frac{dm^2}{\text{ha}}\right) = 0.72 * Basal\ area\ \left(\frac{dm^2}{\text{ha}}\right)$$

Sap flow of tree PFTs was then normalized as follow:

$$Sap\ flow\ density\ \left(\frac{kg}{dm^2 * h}\right) = \frac{Sap\ flow\ \left(\frac{\text{kg}}{\text{h}}\right)}{Basal\ sapwood\ area\ \left(\frac{dm^2}{\text{ha}}\right) * Cohort\ area\ (ha)}$$

On the other hand, sap flow of liana PFT was normalized directly with basal area as follow:

$$Sap\ flow\ density\ \left(\frac{kg}{dm^2 * h}\right) = \frac{Sap\ flow\ \left(\frac{\text{kg}}{\text{h}}\right)}{Basal\ area\ \left(\frac{dm^2}{\text{ha}}\right) * Cohort\ area\ (ha)}$$

The reason was that when recording sap flow in the site, lianas were not allowed to be cut for determining sapwood area. An assumption had been made that the total cross-sectional area of lianas was the same as the sapwood area. Although this seems a bit dangerous, it is general practice for sap flow measurement of lianas. After normalizing sap flow, mean values of cohorts with the same PFT were computed. The PFT means of each time step from all the days in dry/wet months were then averaged to show the impacts on variation during the days of the two seasons. In addition, the impacts of sunlight on liana sap flow were also examined by comparing the sap flow variation during a cloudy day (17^{th}) and a sunny day (24^{th}) during the dry season (November) of 2015.

4. Results

4.1. Comparing hydraulic traits of lianas and trees

The t-test results (table 1) show that lianas had significantly higher $P_{tlp,l}$ and $P_{50,x}$ than trees at the same WD range. In addition to $P_{tlp,l}$ and $P_{50,x}$, water potential at full turgor of tree leaf ($P_{0,l}$) and stem ($P_{0,x}$) are also plotted in figure 8 for comparison. The boxplots (Figure 8a) show that liana leaf lost its turgor at the water potential where tree leaf still had full turgor. Moreover, liana stem (Figure 8b) lost 50% of its hydraulic conductivity at the water potential where tree stem still had full turgor, or the conductivity of tree stem was still good. The t-test results also show that lianas had significantly higher $K_{s,sat}$ than trees with similar WD. On the other hand, no significant difference between the photosynthesis trait (i.e. A_{area}) of lianas and trees was found.

Table 1: Results of t-test on four functional traits of lianas and trees

Parameter	$Mean_{tree}$	N_{tree}	$Mean_{liana}$	N_{liana}	p-value	WD range ($g\ cm^{-3}$)
$P_{tlp,l}$ (MPa)	-1.85	121	-1.55	18	0.001	0.33 - 0.74
$P_{50,x}$ (MPa)	-2.28	130	-1.32	24	<0.001	0.22 - 0.74
Ln($K_{s,sat}$ [$kg\ m^{-1}\ s^{-1}\ MPa^{-1}$])	1.04	124	2.62	28	<0.001	0.22 - 0.74
A_{area} ($\mu mol\ m^{-2}\ s^{-1}$)	10.6	166	9.89	21	0.391	0.32 - 0.77

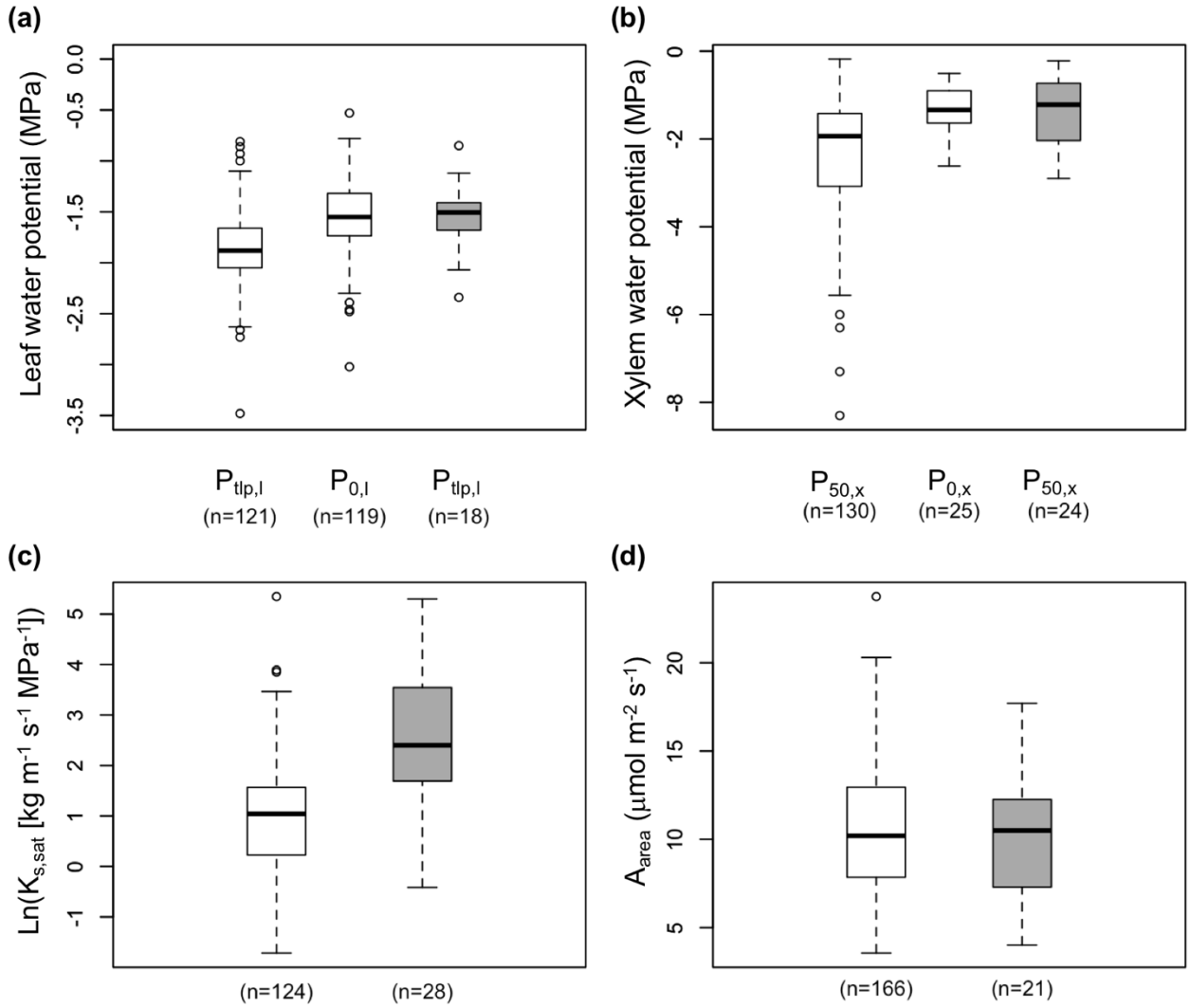

Figure 8: Boxplots of four functional traits (a) $P_{tlp,l}$, (b) $P_{50,x}$,(c) $K_{s,sat}$ and (d) A_{area} of lianas (grey boxes) and trees (white boxes). The plots of water vulnerability traits (a and b) also include water potential at full turgor of tree leaf ($P_{0,l}$) and stem ($P_{0,x}$).

4.2. Linking hydraulic traits of lianas to core traits of stem and leaf

Since the A_{area} was not different between lianas and trees in the same WD range, the parameterization of A_{area} of lianas in ED2 model was implemented using existing development of three PFTs. Therefore, the linear regressions were implemented only for $P_{tlp,l}$, $P_{50,x}$ and $K_{s,sat}$. Step-wise analysis showed no significant interaction effect of SLA and WD on $P_{tlp,l}$ (p-value = 0.141) and SLA was also not a good predictor for $P_{tlp,l}$ (p-value = 0.7). One the other hand, the meta-analysis results of lianas in table 2 show significant correlations (p-value < 0.05) of WD with $K_{s,sat}$ and the absolute value of $P_{tlp,l}$ and $P_{50,x}$. WD as a predictor was able to explain 31, 28.1 and 17.2 percent of the variation in the data of $K_{s,sat}$, $P_{tlp,l}$ and $P_{50,x}$, respectively. Figure 9 illustrates

that the correlation slopes of lianas were quite similar to trees, except for $K_{s,sat}$ data from trees in tropical dry forests (Figure 9c). However, the intercepts were different between lianas and trees leading to that at the same WD the woody vines had higher $K_{s,sat}$ (Figure 9c) and lower absolute values of $P_{tlp,l}$ (Figure 9a) and $P_{50,x}$ (Figure 9b).

Table 2: Resulted linear models from meta-analysis for lianas

Linear model	p-value	r^2	N
$Ln(-P_{tlp,l}$ [MPa]) = 0.521 * Ln(WD [g cm^{-3}]) + 0.767	0.024	0.281	18
$Ln(-P_{50,x}$ [MPa]) = 1.18 * Ln(WD [g cm^{-3}]) + 0.986	0.044	0.172	24
$Ln(K_{s,sat}$ [kg m^{-1} s^{-1} MPa^{-1}]) = -5.49 * WD [g cm^{-3}] + 5.18	0.002	0.310	28

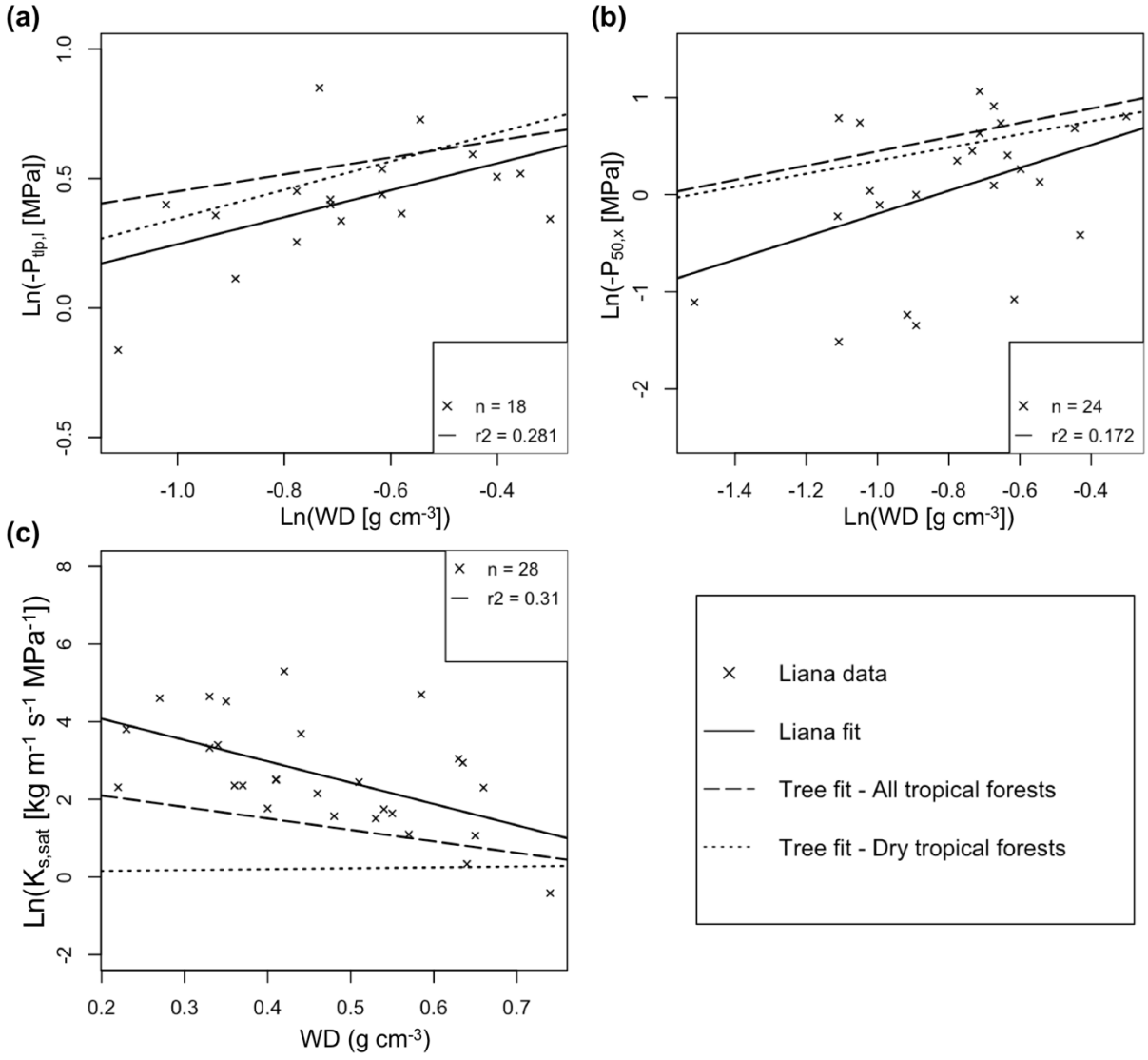

Figure 9: Linear regressions between WD and three hydraulic traits (a) $P_{tlp,l}$, (b) $P_{50,x}$ and (c) $K_{s,sat}$

of lianas (solid lines), trees from all tropical forests (dashed lines) derived from the reconstructed database of Christofferense et al. (2016) and trees from dry tropical forests (dotted lines) derived from the database of Xu et al. (2016). The data points of lianas (x-marks) are also shown, while only the fits are given for trees.

4.3. Model experiment

a) Long-term simulation from bare ground

The results of long-term experimental simulation are plotted in figures 10, 11, 12 and 13. In general, total AGB (Figure 10a) rose drastically during the first 150 years and still increased gradually afterward. Early PFT (Figure 10c) strongly dominated in the beginning with high AGB and was then replaced by mid and late PFTs. The AGB of mid PFT (Figure 10d) was varying around 1-2 kg_C/m^2. Meanwhile, late PFT (Figure 10e) increased rapidly during the first 150 years and became the most dominant in later period. The AGB of lianas (Figure 10b) was little and steady throughout the time. Figure 10c also shows that the AGB of early PFT significantly declined with the presence of lianas leading to a reduction of about 3 kg_C/m^2 in total AGB. The AGB of mid species was also negatively affected by lianas during the period 1750-1950. Although the new hydraulic parameters (dotted lines) did not have an impact on the AGB of liana PFT itself, they affected late PFT causing the AGB slightly higher since 1800.

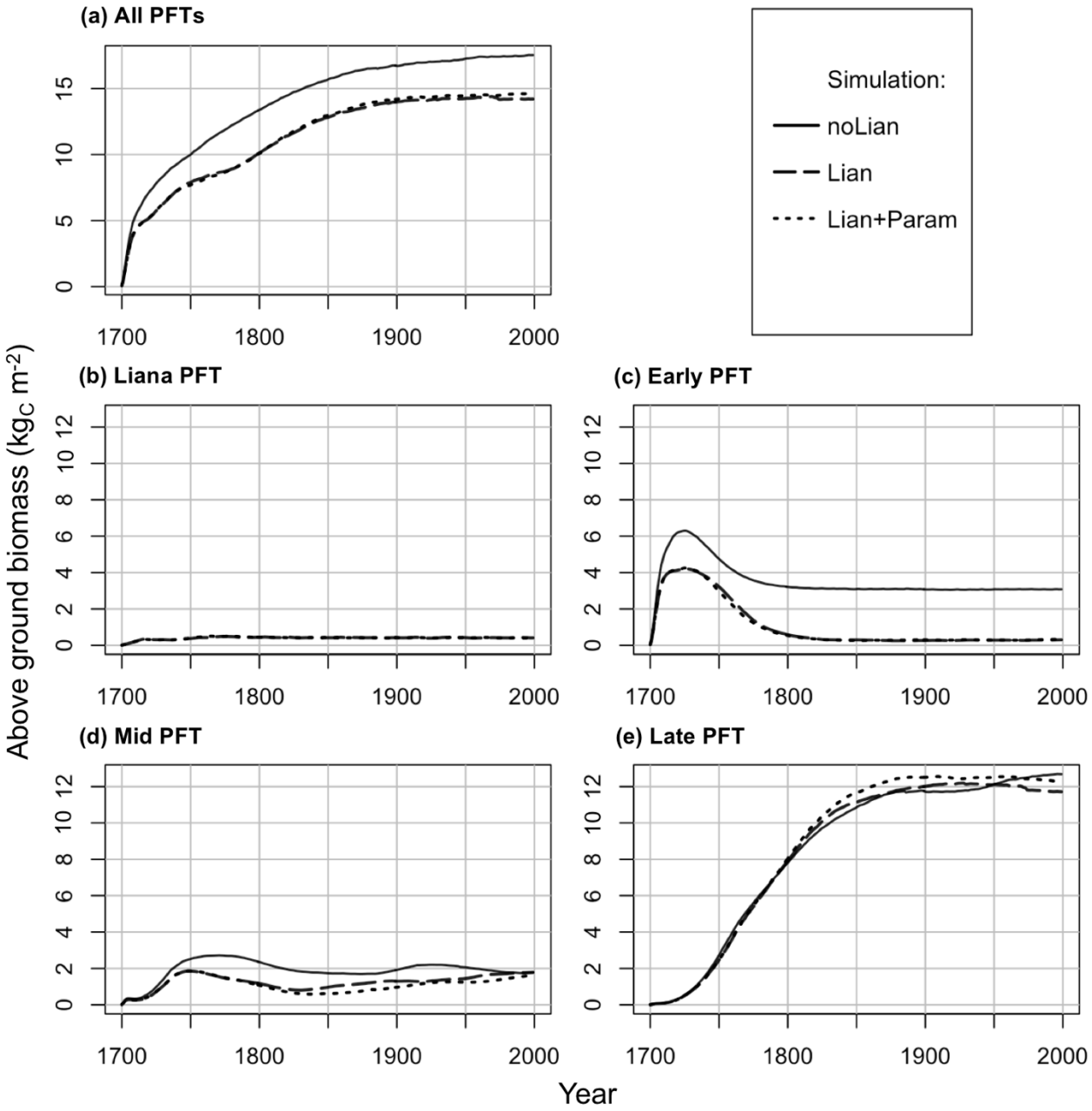

Figure 10: Long-term simulation of total AGB for all PFTs (a), and for liana (b), early (c), mid (d) and late (e) PFTs. For each PFT, the results of three simulation setups noLian (solid lines), Lian (dashed lines) and Lian+Param (dotted lines) are also shown.

Total leaf biomass and leaf biomass of four PFTs (Figure 11) had quite similar trend with their AGB, though they peaked sooner, only after around 50 years. Despite having little AGB, liana PFT (Figure 11b) had relatively high leaf biomass which was higher than both early and mid PFTs (Figure 11c and 11d) when it presented. It can also be seen that leaf biomass of early and mid PFTs significantly decreased with the presence of lianas leading to a small reduction in total leaf

biomass (Figure 11a). However, the new liana parameters did not have any significant impact on the simulation of leaf biomass.

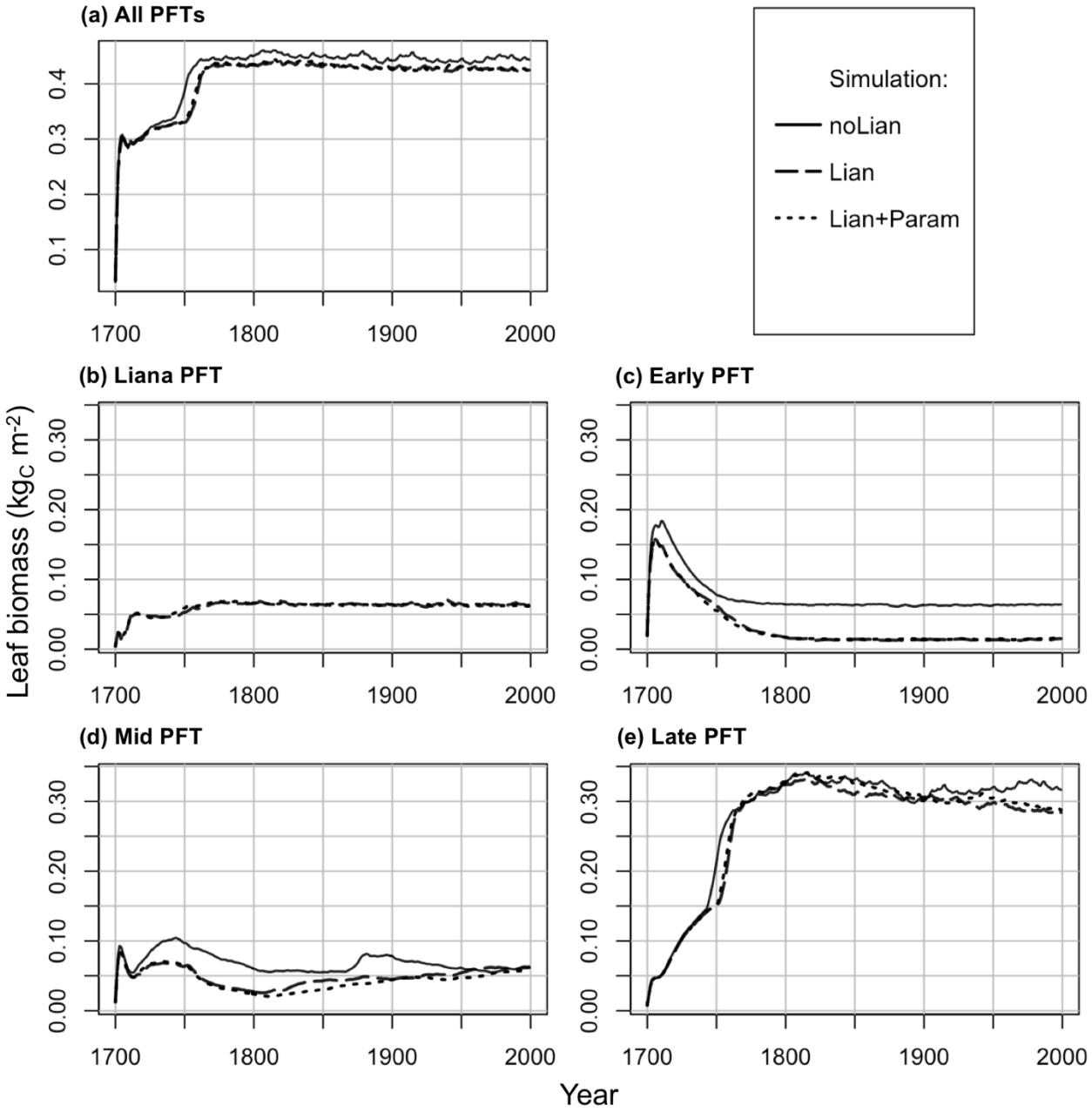

Figure 11: Long-term simulation of total leaf biomass for all PFTs (a), and for liana (b), early (c), mid (d) and late (e) PFTs. For each PFT, the results of three simulation setups noLian (solid lines), Lian (dashed lines) and Lian+Param (dotted lines) are also shown.

The storage biomass of mid and late PFTs (Figure 12d and 12e) were stable throughout the years. Meanwhile, the storage biomass of early species (Figure 12c) became steady after an early peak. Currently, the implementation of the liana biomass storage (Figure 12b) in the model is not quite realistic as lianas put relatively large amount of carbon into the storage pool. However, the presence of lianas still negatively affected the storage biomass of early PFT.

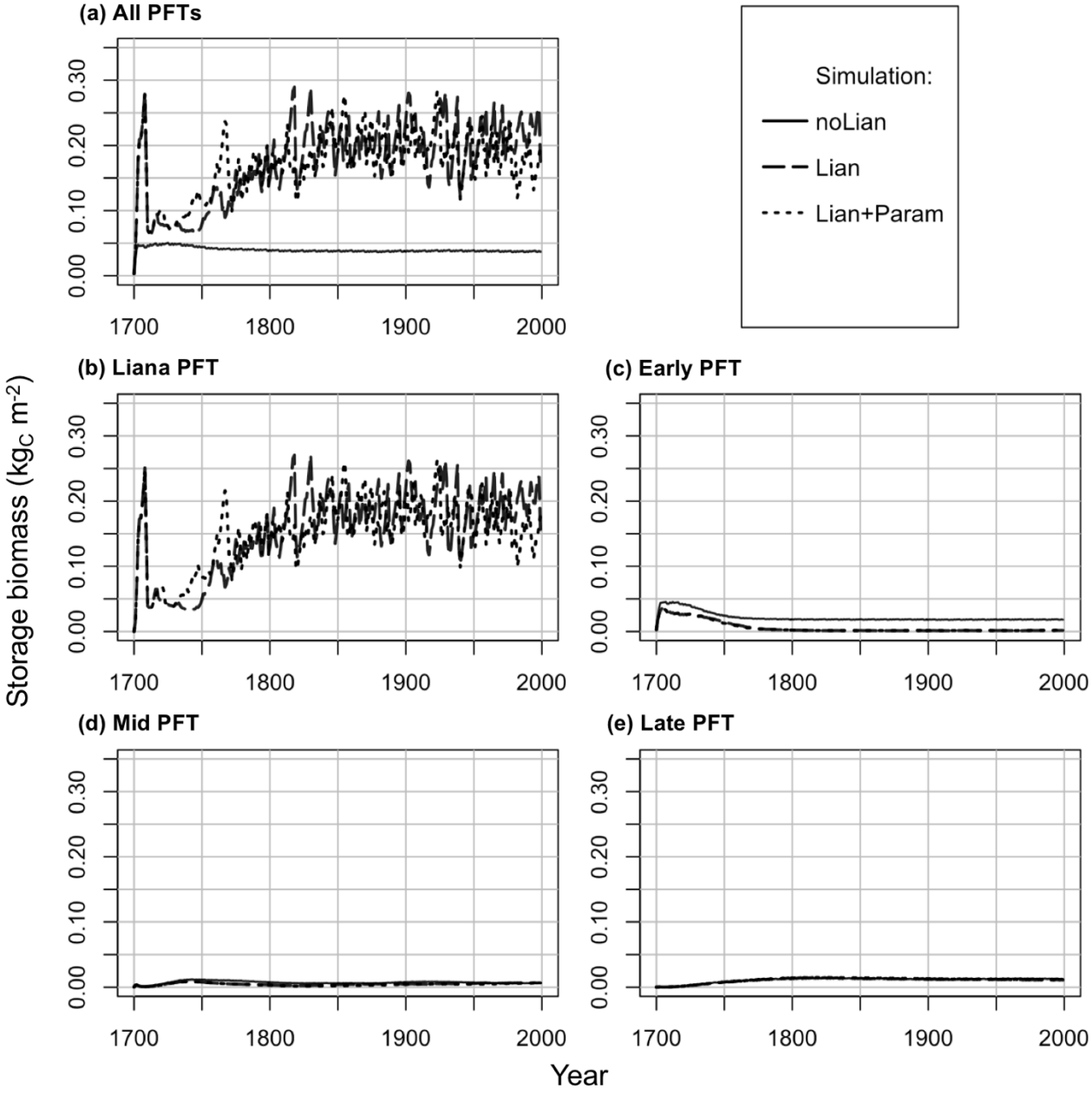

Figure 12: Long-term simulation of total storage biomass for all PFTs (a), and for liana (b), early (c), mid (d) and late (e) PFTs. For each PFT, the results of three simulation setups noLian (solid lines), Lian (dashed lines) and Lian+Param (dotted lines) are also shown.

Figure 13 shows that total leaf transpiration (Figure 13a) peaked after several years together with the peak of early PFT (Figure 13c), and then gradually decreased and became stable with the reduction of early PFT. In general, leaf transpiration of liana, early, mid and late PFTs had quite similar trend with AGB and leaf biomass. Liana and late PFTs (Figure 13b and 13e) both contributed significantly (more than 25%, each) to total transpiration. This was substantially more than early and mid PFTs (Figure 13c and 13d). It also can be seen that the presence of lianas significantly reduced leaf transpiration of early and mid (for a certain period) PFTs. Finally, the new liana parameters did not have any significant impact on the simulation of leaf transpiration.

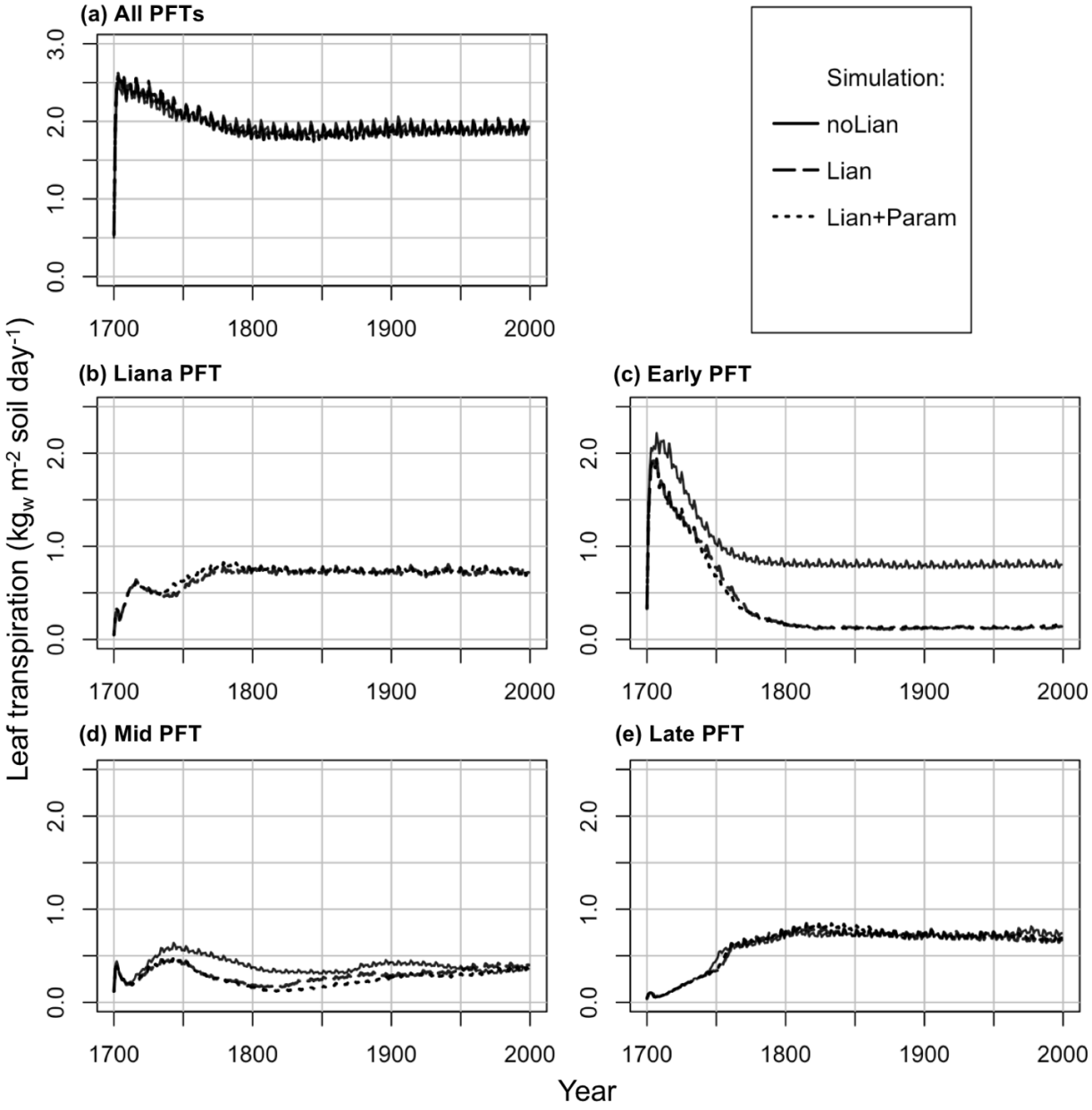

Figure 13: Long-term simulation of total leaf transpiration for all PFTs (a), and for liana (b), early

(c), mid (d) and late (e) PFTs. For each PFT, the results of three simulation setups noLian (solid lines), Lian (dashed lines) and Lian+Param (dotted lines) are also shown.

b) Wet season vs. dry season simulation

The results of seasonal experimental simulation are plotted in figures 14, 15 and 16. In general, total leaf transpiration (Figure 14) during the wet month was lower than during the dry month. The transpiration was peak during midday (from 12:00 to 14:00) and did not occur during the night. The highest leaf transpiration during midday was from early successional PFT without the competition of lianas (Figure 14b) and the lowest was from mid successional PFT (Figure 14c). The leaf transpiration of lianas (Figure 14a) was similar to late PFT (Figure 14d) when they presented. On the other hand, leaf transpiration of early and late PFTs fell dramatically with the presence of lianas (dashed and dotted lines). For early PFT, the reduction was around 80%. Figure 14c also illustrates that leaf transpiration of mid PFT slightly declined during midday in the simulation with new liana parameters (dotted lines).

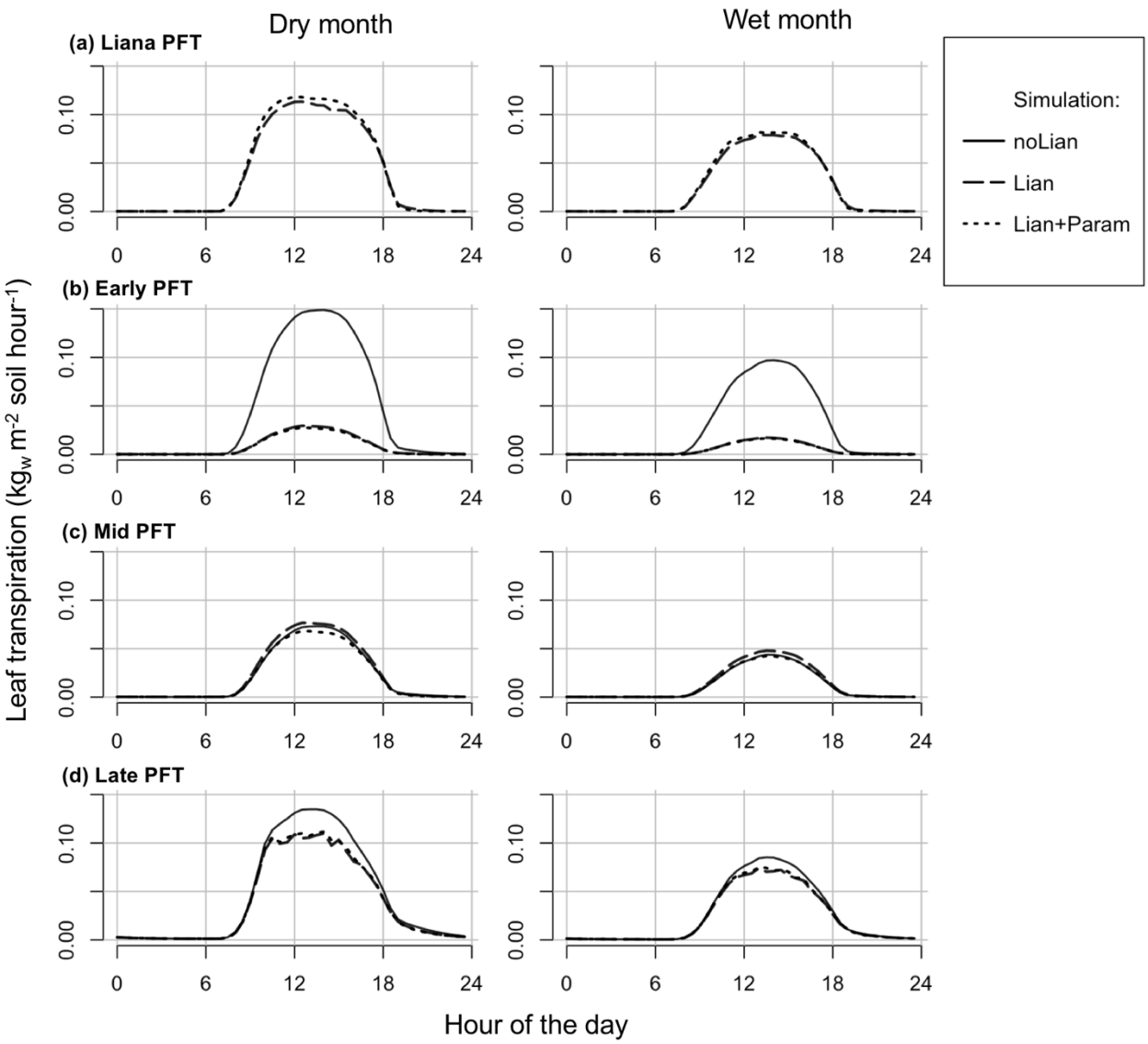

Figure 14: Variation during the day in dry month (September 2009) and wet month (April 2010) of total leaf transpiration from liana (a), early (b), mid (c) and late (d) PFTs. For each PFT, the results of three simulation setups noLian (solid lines), Lian (dashed lines) and Lian+Param (dotted lines) are also shown.

Ψ_L (Figure 15) in wet month was less negative than during the dry month. It also can be seen that Ψ_L was most negative from 12:00 to 18:00 and was less negative during the night. The most negative Ψ_L was from late PFT (Figure 15d) followed by lianas in the simulation without specific parameters (Figure 15a) and mid and early PFTs (Figure 15c and 15b), respectively. Figure 15a and 15c illustrates that Ψ_L of lianas with specific hydraulic parameters was similar to that of mid PFT. During midday, Ψ_L of early and mid PFTs and lianas with specific hydraulic parameters

were higher than $P_{tlp,l}$, while late PFT and lianas without specific parameters had Ψ_L lower than $P_{tlp,l}$. Therefore, the new parameters significantly affected Ψ_L of lianas during midday. On the other hand, the presence of lianas strongly reduced Ψ_L of late PFT.

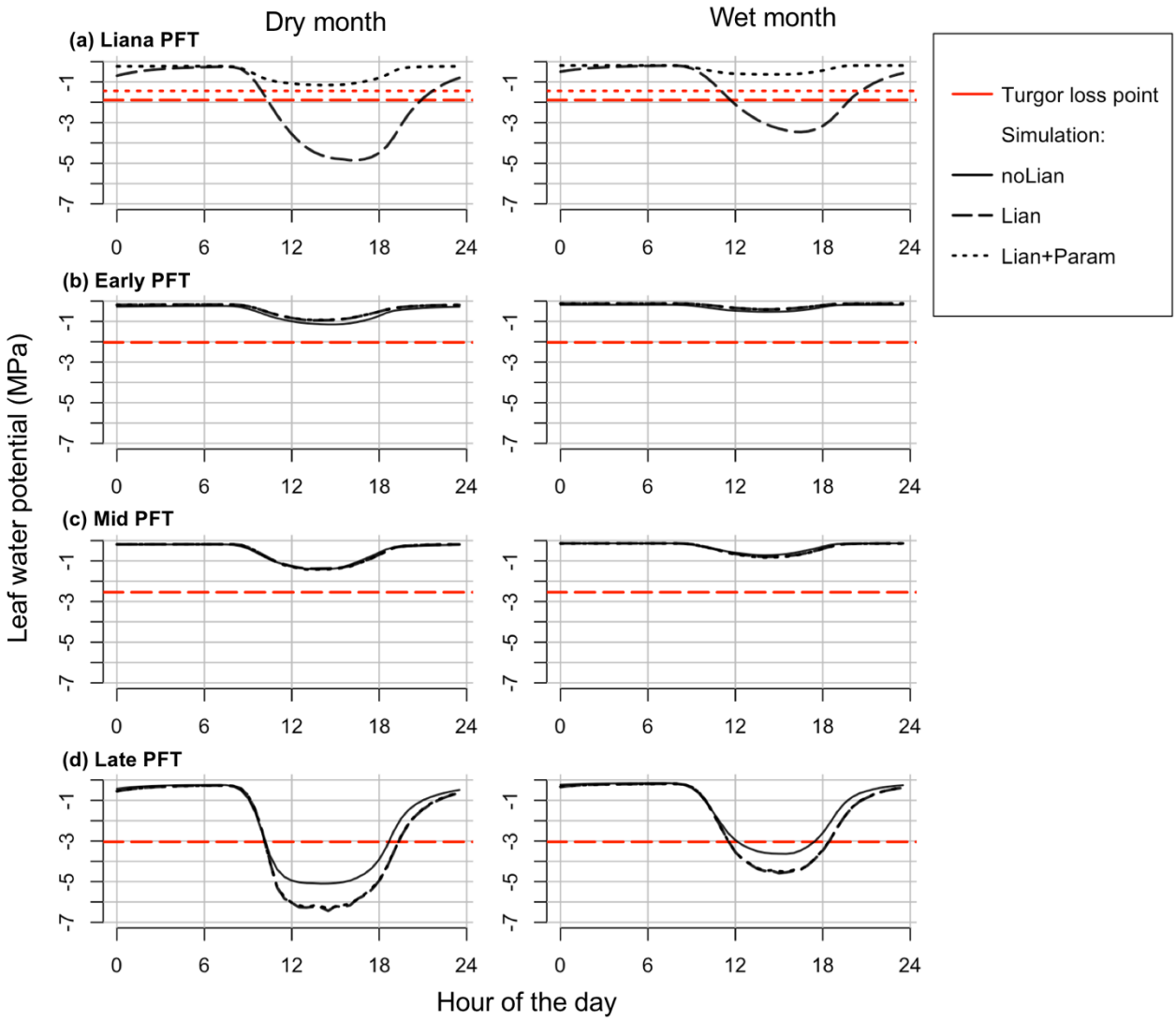

Figure 15: Variation during the day in dry month (September 2009) and wet month (April 2010) of Ψ_L from liana (a), early (b), mid (c) and late (d) PFTs. The corresponding $P_{tlp,l}$ with each PFT are also plotted (red dashed lines). For each PFT, the results of three simulation setups noLian (black solid lines), Lian (black dashed lines) and Lian+Param (black dotted lines) are also shown. Note that for lianas there are two lines of $P_{tlp,l}$, one from setup Lian parameterized by existing development of trees (red dashed lines) and one from setup Lian+Param parameterized by the results of meta-analysis (red dotted lines).

Both setups Lian and Lian+Param resulted in a strong variation in daily Ψ_L of lianas (Figure 16a) throughout the dry month. Simulation Lian+Param (blue line) with new parameters, however, generated a clear decreasing trend of Ψ_L of lianas throughout the dry period. The correlation between Ψ_{pd} and Ψ_{md} plotted on figure 16c also supported this trend. On the other hand, without lianas specific parameters (black line) the variation of Ψ_L was much more significant during the day with extremely low Ψ_{md}. However, the decreasing trend of this simulation during the dry month was not clear. The slope of the correlation between Ψ_{pd} and Ψ_{md} (Figure 16b) was also significantly smaller (flatter) than simulation of lianas with new hydraulic parameters.

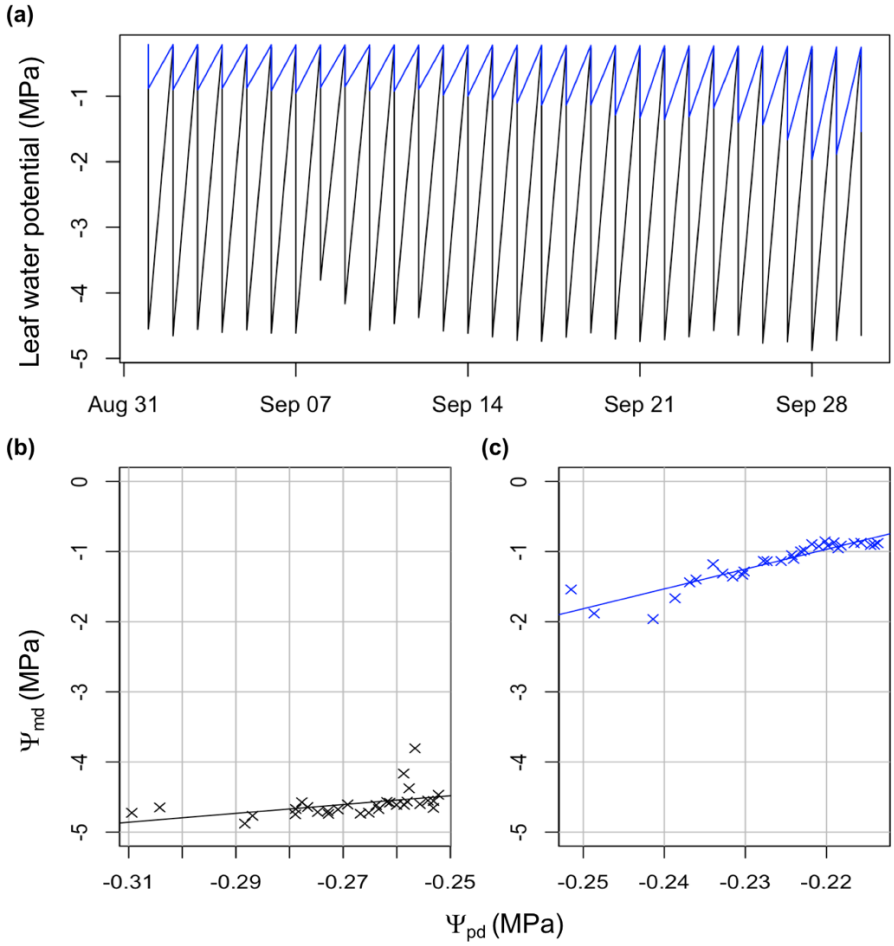

Figure 16: Weighted mean of Ψ_{pd} and Ψ_{md} of lianas in September 2009 from two simulation setups Lian (black line) and Lian+Param (blue line) plotted in series (a). Linear correlations between these Ψ_{pd} and Ψ_{md} from the two simulation setups Lian (b) and Lian+Param (c) are also shown.

4.4. Model evaluation

a) Evapotranspiration simulation

The results of evapotranspiration simulation are shown in figures 17, 18 and 19. In general, the evapotranspiration (Figure 17) was peak during midday (from 12:00 to 14:00) and was minimal during the night. Figure 17 also demonstrates a higher observation of total evapotranspiration in the dry month than in the wet month. Although all three simulation setups were able to catch the diurnal trend, they generated no significant difference between the seasons. This lead to underestimation and overestimation of evapotranspiration during the dry and wet months, respectively. Among the simulation setups, evapotranspiration declined with the presence of lianas (black dashed and black dotted lines).

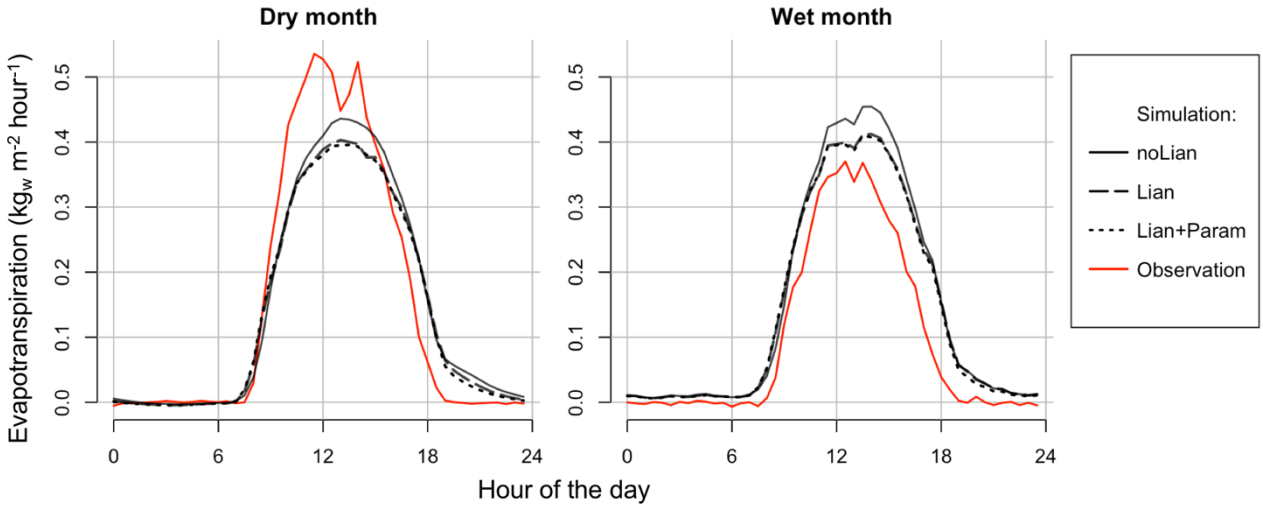

Figure 17: Variation during the day in dry month (September 2009) and wet month (April 2010) of total evapotranspiration from three simulation setups including noLian (black solid line), Lian (black dashed line) and Lian+Param (black dotted line) versus observation (red solid line).

Figure 18 shows that total evapotranspiration peaked around the dry period (from July to September) and decreased during the rainy period (from December to February). All the simulations were able to catch this trend, though the variation during the year was smaller and they tended to overestimate the monthly means of total evapotranspiration. The presence of lianas, however, decreased this overestimation. Figure 17 and 18 also show very little impact of the new liana parameters (black dotted lines) on both hourly and monthly mean of total evapotranspiration.

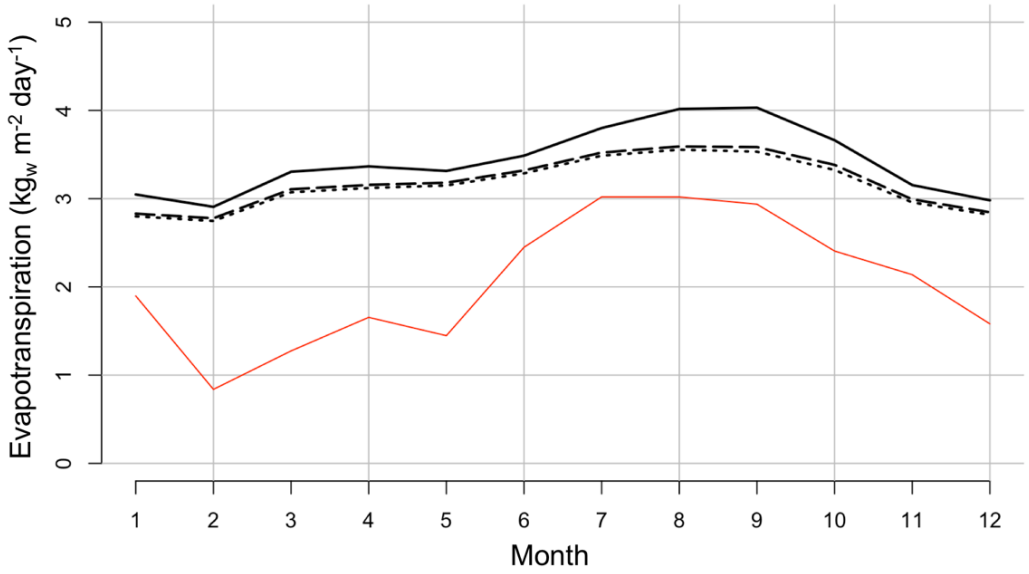

Figure 18: Monthly means of total evapotranspiration in 2016 from three simulation setups including noLian (black solid line), Lian (black dashed line) and Lian+Param (black dotted line) versus observation (red solid line).

Both the simulation and observation of total evapotranspiration (Figure 19) decreased over the years (from 2005 to 2016). Although all simulations tended to overestimate the yearly means of total evapotranspiration, the presence of lianas decreased this overestimation. Moreover, the new hydraulic parameters of lianas (black dotted line) resulted in the lowest yearly means and therefore, slightly improved the model simulation.

Figure 19: Yearly means of total evapotranspiration from three simulation setups including noLian

(black solid line), Lian (black dashed line) and Lian+Param (black dotted line) versus observation (red solid line).

b) Sap flow simulation

The results of sap flow simulation are shown in figures 20 and 21. In general, sap flow (Figure 20) during the wet month was slightly lower than during the dry month. When there were no lianas, the midday sap flow was highest of late PFT (Figure 20d) followed by mid and early PFTs (Figure 20c and 20b), respectively. When lianas presented, they (Figure 20a) had the highest midday sap flow followed by early, late and mid PFTs, respectively. This domination of lianas significantly reduced the sap flow of mid and late PFTs while promoted the sap flow of early PFT. On the other hand, the highest observed sap flow was also of lianas, however, was followed by mid, early and late PFTs, respectively. The observation also showed that sap flow was peaking around midday (12-14h) and did not occur during the night except for lianas and mid PFT. It can be seen that the model tended to underestimate the midday sap flow, except for midday sap flow of late PFT which was substantially overestimated. The new hydraulic parameters of lianas (black dotted lines) resulted in higher peaks during midday of liana sap flow and therefore were more similar to the observation.

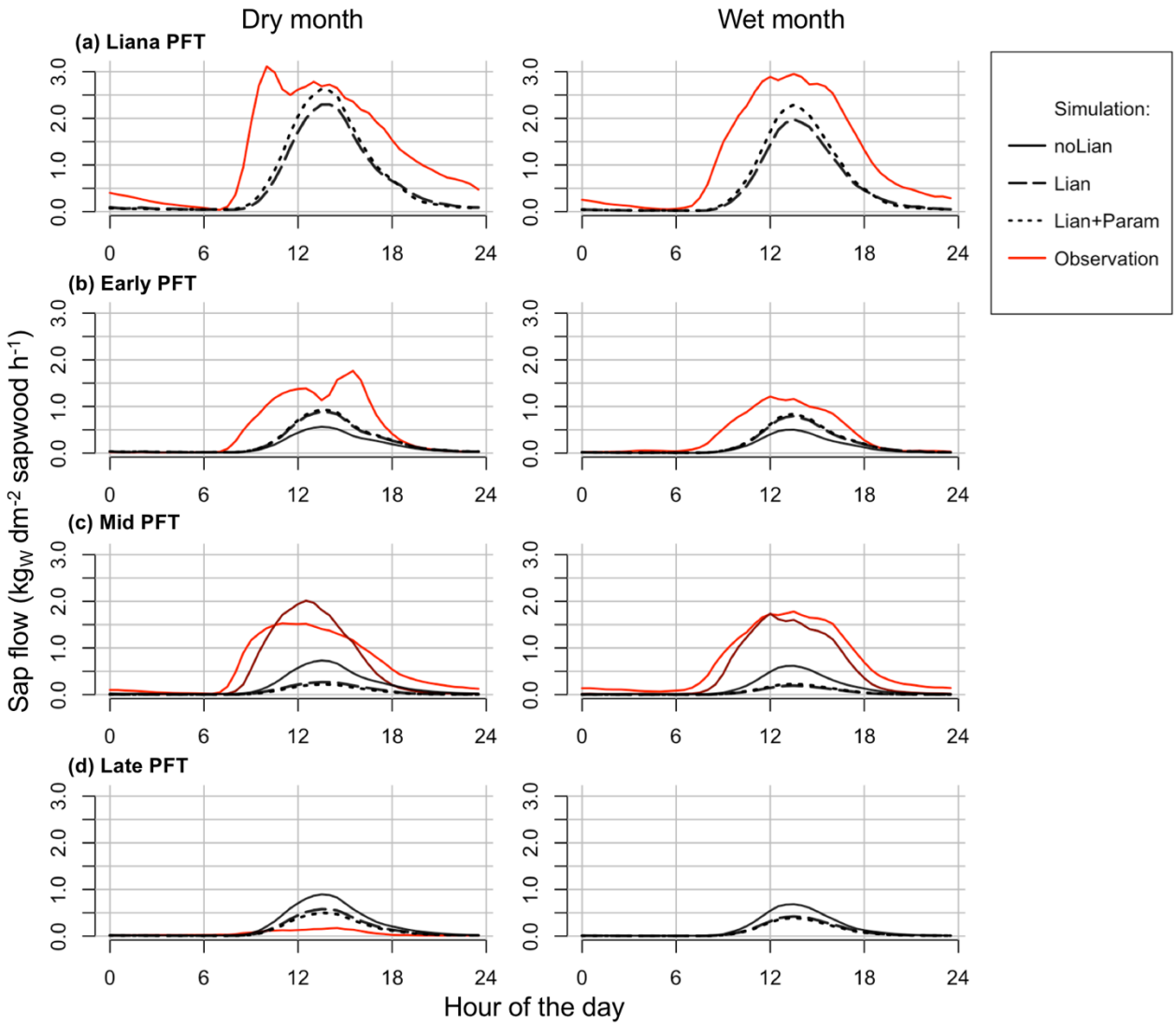

Figure 20: Variation during the day in dry months (November 2015 and January 2016) and wet months (April and May 2016) of mean sap flow from liana (a), early (b), mid (c) and late (d) PFTs. The corresponding observations (Liana species versus liana PFT, Sloanea sp. versus early PFT, G. glabra and O. asbeckii versus mid PFT, and L. membranacea versus late PFT) are plotted (red and dark red solid lines). For each PFT, the results of three simulation setups noLian (black solid lines), Lian (black dashed lines) and Lian+Param (black dotted lines) are also shown.

Figure 21a illustrates that on the clear day, photosynthesis active radiation (PAR) peaked once at midday (around 12:00), while PAR reached several peaks during the cloudy day. The impacts of PAR on liana sap flow (Figure 21b) can be clearly seen on the cloudy day. The midday peak of observed sap flow was impeded and broken down to several small peaks. The simulations with or without new liana parameters both generated liana sap flow that was quite similar to the

observation on the clear day. However, the model setup Lian (black dashed lines) resulted in more realistic sap flow with a second and a third peak that associated with observed PAR during the cloudy day. Therefore, simulation of Lian was better at capturing the impacts of PAR on sap flow.

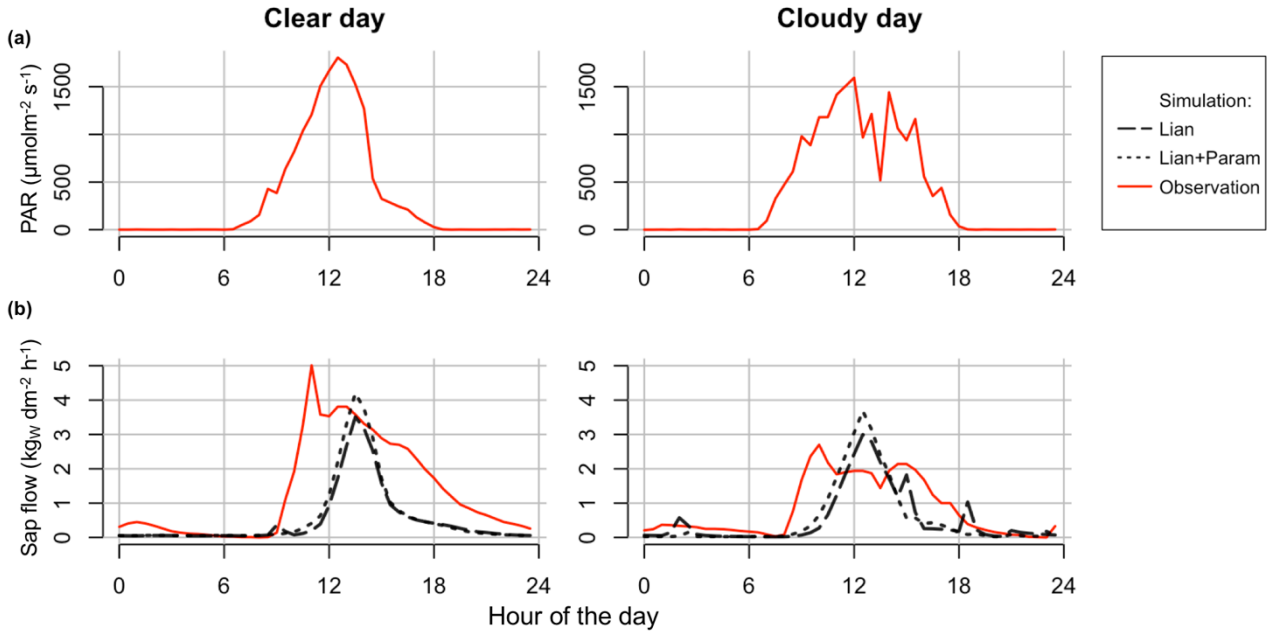

Figure 21: Variation during a clear day and a cloudy day in the dry month (November 2015) of observed PAR (a), and mean liana sap flow (b) from observation (red solid line) and two simulation setups Lian (black dashed line) and Lian+Param (black dotted line).

5. Discussion

5.1. Comparing hydraulic traits of lianas and trees

There was limited data on liana hydraulic traits among the community as the number of records found was smaller than 30 for each of the traits. However, the limited records still showed that lianas had a wide WD range of lianas (0.22 – 0.74 g/cm^3) that could be comparable with trees. This finding supports the previous studies of van der Sande et al. (2013) and De Guzman et al. (2016) that contradict the expected low WD of the woody vines. Although having similar WD, lianas were still associated with a riskier water-use strategy compared with trees. The climbers let themselves to be more vulnerable to water stress with substantially high $P_{tlp,l}$ and $P_{50,x}$ in exchange for efficiency in water transport with a high $K_{s,sat}$ (Table 1). This trade-off was also found in previous studies (Zhu & Cao, 2009; De Guzman, et al., 2016; Chen, et al., 2017). However, the meta-analysis showed for the very first time that lianas have to pay a great price for their water transport efficiency. At the water potential where tree leaves and stems were able to maintain their full turgor, liana leaves had already lost their turgor and liana stems had lost 50% of their hydraulic conductivity (Figure 8a and 8b). In contrast, $K_{s,sat}$ of lianas was roughly 4 times larger than the $K_{s,sat}$ of trees (Figure 8c). According to Chen et al. (2017), this trade-off, which seems to be dangerous during the drought period, is actually their water-use strategy for dealing with water deficits. The reason is that despite losing almost half of the conductivity during midday, the woody vines still transport water efficiently due to their natural substantial conductivity. On the other hand, photosynthesis capacity between lianas and trees was comparable (Table 1). This is also consistent with earlier studies of Cai et al. (2009) and Slot & Winter (2017).

5.2. Linking hydraulic traits of lianas to core traits of stem and leaf

Unlike trees (Xu, et al., 2016), SLA of lianas was not a good predictor of $P_{tlp,l}$. On the other hand, the significant correlations between liana WD and $K_{s,sat}$, $P_{tlp,l}$ and $P_{50,x}$ (Table 2) prove that the climbers also follow the plant economic spectrum. The similar slopes between liana and tree correlations (Figure 9) illustrates a trade-off between drought tolerance and water transport efficiency along the WD gradient of liana community themselves. As liana WD decreased, their absolute values of $P_{tlp,l}$ and $P_{50,x}$ also decreased meaning that they had less negative $P_{tlp,l}$ and $P_{50,x}$ which are associated with drought vulnerability. However, lianas with low WD had high $K_{s,sat}$ which are associated with water transport efficiency. On the other hand, the differences in correlation intercepts in figure 9 prove that the trade-off found between lianas and trees was not due to an expected low WD of lianas but rather due to natural differences between the growth

forms. At any point along the WD gradient, lianas had higher $K_{s,sat}$ and absolute values of $P_{tlp,l}$ and $P_{50,x}$ than trees meaning that the woody vines were more vulnerable to water-stress but had a higher water transport efficiency. The results of this meta-analysis show substantial differences between lianas and trees and therefore, it is essential to develop independent parameters for lianas.

5.3. Model experiment

a) Long-term simulation from bare ground

In general, all the long-term simulations were able to capture realistically forest demography along the successional gradient of early, mid and late plant types. The results confirm previous studies that lianas could significantly impact forest biomass. Moreover, lianas contributed substantially to forest transpiration (Figure 13), even more than the finding of Restom & Nepstad (2001) which was 9 to 12% of the entire forest transpiration. The simulations also reveal a strong competition between lianas and early species leading to a reduction in the biomass of early PFT. The new hydraulic parameters of lianas did not have a strong impact on long-term simulation. This was expected since the new parameters only brought a minor change to the model with three adjustments in liana hydraulic traits. Furthermore, the site is moist tropical forest with limited drought-stress so that the new drought-vulnerable traits should not strongly affect the yearly mean outputs resulted from long-term simulation. Unlike tree species, leaf biomass of lianas accounted for most of their AGB (Figure 10 and 11). This could be explained by that lianas do not need to allocate most of their resources to structural support like trees. Therefore, despite having a low AGB, lianas had substantial high leaf biomass which allowed them to achieve high leaf transpiration and contribute significantly to whole forest transpiration. On the other hand, the storage biomass of lianas in the current model version was not realistic (Figure 12b). Lianas put to the storage pool around 0.2 kg_C/m^2 significantly higher than total storage biomass of other tree species which was about 0.05 kg_C/m^2. However, with the total reduction of AGB up to 3 kg_C/m^2 (Figure 10a), one cannot attribute this total reduction to the problem of liana storage biomass. In the newest version of lianas in ED2 (which was not able to be implemented during the time of this thesis), this storage problem has been refined in a more sophisticated way.

b) Wet season vs. dry season simulation

In general, the simulations of leaf transpiration and water potential during the day were quite realistic. Leaf transpiration is driven by VPD leading to a higher demand during the dry season. This higher demand also expressed in lower Ψ_L during the dry month than during the wet month

(Figure 15). However, the wet conditions of the study site show limited water stress that normally restrains transpiration during the dry season. Thus, high demand without any constraint resulted in higher leaf transpiration during the dry month than during the wet month (Figure 14). Similar to long-term simulation, leaf transpiration of lianas during the day was substantial (Figure 14a). The presence of lianas significantly reduced the transpiration of early and late tree types (Figure 14b and 14d). Moreover, the decrease in Ψ_L of late species (Figure 15d) implied a strongly below-ground competition with lianas for water resources. Given the significant impacts of lianas on both long-term and seasonal simulations, it is vital to implement lianas in the next generation of DGVMs.

On the other hand, the new hydraulic parameters significantly impacted Ψ_L of lianas (Figure 15a). In the simulation with specific hydraulic parameters, the climbers did not lose leaf turgor during the day and therefore, they maintained their full physiological functions of leaf such as photosynthesis and transpiration. This should give lianas a major advantage in competition with other PFTs, especially late PFT. The model setup with new hydraulic parameters also simulated a clearly decreasing trend of Ψ_L of lianas throughout the dry period. According to Werden et al. (2017), plants regulate Ψ_L using two main water-use strategies. Isohydric plants (drought-avoiders) maintain approximately constant Ψ_L by regulating the opening and closure of their stomata. Meanwhile, anisohydric plants (drought-tolerators) keep their stomata open and allow Ψ_L to decline. Lianas with new parameters clearly behaved like an anisohydric plant (Figure 16a and 16c) which is consistent with the findings of Werden et al. (2017). This water-use strategy of lianas benefits them when under wet or even moderately stressful conditions, though it might endanger the climbers under intense drought (Sade, et al., 2012).

5.4. Model evaluation

a) Evapotranspiration simulation

Although the differences in evapotranspiration between dry and wet seasons were poorly represented by ED2 at hourly time-scale (Figure 17), the differences were much better generated at monthly time-scale (Figure 18). All the results show that the incorporation of lianas and their new hydraulic parameters reduced total evapotranspiration. The main reason was due to the drastic decrease in total leaf transpiration of early and late PFTs in the simulation with lianas (Figure 14b and 14d). Substantial leaf transpiration of lianas could not compensate for all of the reduction that they brought. Moreover, the lower total evapotranspiration can be partially explained by the decline in sap flow per sapwood area of mid and late PFTs (Figure 20c and

20d). On the other hand, the yearly evapotranspiration of Lian+Param simulation was a little lower than Lian simulation (Figure 19) due to the slight reduction in total leaf transpiration of mid PFT (Figure 14c). Thus, the incorporation of lianas and their new hydraulic parameters reduced the overestimation of both monthly mean and yearly mean of total evapotranspiration leading to a more realistic simulation. This emphasizes the critical role of including lianas with the specific parameters in DVGMs

b) Sap flow simulation

It was not expected to have a perfect match between simulation and observation of sap flow. The reason was that the sap flow data was species specific (and only measured on a limited number of individuals), while the species diversity in ED2 was aggregated into PFTs. Nonetheless, the model successfully captured the expected significant sap flow of lianas (Figure 20). The higher $K_{s,sat}$ in new hydraulic parameters increased the peak of liana sap flow during the day making the simulation more realistic compared with the observation (Figure 20a). The presence of lianas reduced sap flow of mid and late species which was consistent with the findings of Campanello et al. (2016) shown in figure 1. More importantly, the reduction in late species resulted in the sap flow that was more similar to the observation (Figure 20d). However, liana presence increased the sap flow of early species (Figure 20b). This could be explained by that mid and late species are slow growing trees and therefore, are likelier to be affected by lianas (Campanello, et al., 2016). This impact on mid and late species, on the other hand, promoted the sap flow of early species. This indirect influence of lianas on the competition between tree species was already stated in previous study by Schnitzer & Bongers (2002). Although the individual sap flow of early species raised, their total AGB and leaf transpiration decreased (Figure 10c and 13c) meaning that lianas also strongly competed and reduced the population of early tree species.

The simulation of liana sap flow on clear and cloudy days reveals that the new hydraulic parameters poorly represented the impacts of sunlight on sap flow during the midday (Figure 21). When there is more sunlight, PAR will increase which promotes plant photosynthesize and sap flow. However, PAR could be significantly limited by clouds. The simulation without new parameters (black dashed lines) well captured this cloud impacts because in the parameterization, $K_{s,sat}$ was indirectly linked to A_{max} via $K_{l,max,x}$. The positive correlation between $K_{l,max,x}$ and A_{area} (Christoffersen, et al., 2016) gave ED2 the ability to capture the impacts of sunlight on midday sap flow. Meanwhile, there was no link between $K_{s,sat}$ and A_{area} in the new hydraulic parameterization which explains for the poor simulation of sap flow during cloudy day.

6. Conclusion and recommendation

Lianas have been shown to substantially affect dynamics, carbon sequestration and water cycle of tropical forest ecosystems. However, the mechanisms of these processes are poorly understood. Moreover, the application of DGVMs in studying these processes and mechanisms is being constrained due to the lack of integrating lianas in the current generation of DGVMs. The results of this master thesis, therefore, contribute to the implementation of lianas in a DGVM (e.g. ED2) for the first time.

This research provides solid evidences of a trade-off between drought tolerance and water transport efficiency along the WD gradient of liana community. Meanwhile, a similar trade-off for water transport efficiency found between lianas and trees was not due to a popular expected low WD of the climbers but rather due to natural differences between the growth forms in the same WD range. The research, therefore, shows the importance to develop specific model parameters for lianas.

The implementation of lianas and their hydraulic parameters in ED2 provides insights on the role of lianas in tropical forest ecosystem. The presence of lianas in a tropical moist forest of French Guiana, South America significantly reduced biomass of tree species and total forest biomass. Lianas also contributed substantially to the whole forest transpiration. Moreover, there were evidences that lianas not only competed directly with tree species for water resources but also indirectly influenced the competition among tree species (i.e. PFTs in the simulations). On the other hand, the incorporation of lianas and their hydraulic parameters improved the model performance and generated more realistic simulations of e.g. evapotranspiration, sap flow and liana water-use strategy.

Overall, the research shows the critical role of lianas in the water cycle of tropical forest ecosystem and therefore, indicates the importance of incorporating lianas in tropical forest modelling.

For future research on tropical forest modelling, it is recommended to include lianas at least in an implicit way. The presence of lianas is prerequisite for a realistic water cycle simulation. It is also suggested to link $K_{s,sat}$ to A_{area} to improve sap flow simulation for the next development of liana PFT. On the other hand, there are needs for more studies on lianas since the knowledge and data of the climbers are still limited.

7. References

Aubinet, M. et al., 1999. Estimates of the Annual Net Carbon and Water Exchange of Forests: The EUROFLUX Methodology. *Advances in Ecological Research,* Volume 30, pp. 113-175.

Avalos, G., Mulkey, S., Kitajima, K. & Wright, S. J., 2007. Colonization Strategies of Two Liana Species in a Tropical Dry Forest Canopy. *Biotropica,* 39(3), pp. 393-399.

Bartlett, M. K., Scoffoni, C. & Sack, L., 2012. The determinants of leaf turgor loss point and prediction of drought tolerance of species and biomes: a global meta-analysis. *Ecology Letters,* 15(5), p. 393–405.

Bartlett, M. K. et al., 2014. Global analysis of plasticity in turgor loss point, a key drought tolerance trait. *Ecology Letters,* Issue 17, pp. 1580-1590.

Bonal, D. et al., 2008. Impact of severe dry season on net ecosystem exchange in the Neotropical rainforest of French Guiana. *Global Change Biology,* Volume 14, pp. 1917-1933.

Brenes-Arguedas, T., Roddy, A. & Kursar, T., 2013. Plant traits in relation to the performance and distribution of woody species in wet and dry tropical forest types in Panama. *Functional Ecology,* 27(2), p. 392–402.

Cai, Z.-q. & Bongers, F., 2007. Contrasting Nitrogen and Phosphorus Resorption Efficiencies in Trees and Lianas from a Tropical Montane Rain Forest in Xishuangbanna, South-West China. *Journal of Tropical Ecology,* 23(1), pp. 115-118.

Cai, Z.-Q., Schnitzer, S. A. & Bongers, F., 2009. Seasonal Differences in Leaf-Level Physiology Give Lianas a Competitive Advantage over Trees in a Tropical Seasonal Forest. *Oecologia,* 161(1), pp. 25-33.

Campanello, P. I. et al., 2016. Carbon Allocation and Water Relations of Lianas Versus Trees. *Tropical Tree Physiology,* Volume 6, pp. 103-124.

Carvalho, E. C. D. et al., 2016. Why is liana abundance low in semiarid climates?. *Austral Ecology,* 41(5), p. 559–571.

Carvalho, E. C. D. et al., 2015. Hydraulic architecture of lianas in a semiarid climate: efficiency or safety?. *Acta Botanica Brasilica,* 29(2), pp. 198-206.

Castanho, A. D. A. et al., 2013. Improving simulated Amazon forest biomass and productivity by including spatial variation in biophysical parameters. *Biogeosciences,* Volume 10, p. 2255–2272.

Chapin III, F. S., Matson, P. A. & Mooney, H. A., 2002. Chapter 4: Terrestrial Water and Energy Balance. In: sd, ed. *Principles of Terrestrial Ecosystem Ecology.* New York: Springer-Verlag New York, Inc, pp. 71-96.

Chave, J. et al., 2009. Towards a worldwide wood economics spectrum. *Ecology Letters,* 12(4), pp. 351-366.

Chen, Y.-j.et al., 2014. Different biomechanical design and ecophysiological strategies in juveniles of two liana species with contrasting growth habit. *American Journal of Botany,* 101(6), p. 925–934.

Chen, Y.-J.et al., 2015. Water-use advantage for lianas over trees in tropical seasonal forests. *New Phytologist,* 205(1), p. 128–136.

Chen, Y.-J.et al., 2017. Physiological regulation and efficient xylem water transport regulate diurnal water and carbon balances of tropical lianas. *Functional Ecology,* Volume 31, p. 306–317.

Chiu, S.-T. & Ewers, F. W., 1992. Xylem structure and water transport in a twiner, a scrambler, and a shrub of Lonicera (Caprifoliaceae). *Trees (Berl),* Volume 6, pp. 216-224.

Choat, B. et al., 2012. Global convergence in the vulnerability of forests to drought. *Nature,* Volume 491, p. 752–755.

Christoffersen, B. O. et al., 2016. Linking hydraulic traits to tropical forest function in a size-structured and trait-driven model (TFS v.1-Hydro). *Geoscientific Model Development,* Volume 9, pp. 4227-4255.

De Guzman, M. E., Santiago, L. S., Schnitzer, S. A. & Álvarez-Cansino, L., 2016. Trade-offs between water transport capacity and drought resistance in neotropical canopy liana and tree species. *Tree Physiology,* Volume 00, pp. 1-11.

Deurwaerder, H. D. et al., 2018. Liana and tree below-ground water competition - evidence for water resource partitioning during the dry season. *Tree Physiology,* 0(0), pp. 1-13.

Ewers, F. W. & Fisher, J. B., 1991. Why vines have narrow stems: histological trends in Bauhinia (Fabaceae). *Oecologia,* Volume 88, pp. 233-237.

Ewers, F. W., Fisher, J. B. & Chiu, S.-T., 1990. A survey of vessel dimensions in stem of tropical lianas and other growth forms. *Oecologia,* Volume 84, pp. 544-552.

Ewers, F. W., Rosell, J. & Olson, M., 2015. Lianas as structural parasite. In: U. Hacke, ed. *Functional and ecological xylem anatomy.* New York: Springer, p. 163–188.

FAO, 1998. *Crop evapotranspiration - Guidelines for computing crop water requirements.* Rome: Food and Agriculture Organization of the United Nations.

FAO-ISRIC-ISSS, 1998. *World reference base for soil resources,* Rome, Italy: World Soil Resources Report 84, Food and Agriculture Organization of the United Nations.

Feild, T. et al., 2012. The evolution of angiosperm lianescence without vessels – climbing mode and wood structure–function in Tasmannia cordata (Winteraceae). *The New Phytologist,* 193(1), pp. 229-240.

Feild, T., Chatelet, D. S. & Brodribb, T., 2009. Ancestral xerophobia: a hypothesis on the whole plant ecophysiology of early angiosperms. *Geobiology,* 7(2), p. 237–264.

Feild, T. & Isnard, S., 2013. Climbing Habit and Ecophysiology of Schisandra glabra (Schisandraceae): Implications for the Early Evolution of Angiosperm Lianescence. *International Journal of Plant Sciences,* 174(8), pp. 1121-1133.

Field, T. S. & Balun, L., 2008. Xylem hydraulic and photosynthetic function of Gnetum (Gnetales) species from Papua New Guinea. *New Phytol,* Volume 177, pp. 665-675.

Fisher, R. et al., 2010. Assessing uncertainties in a second-generation dynamic vegetation model caused by ecological scale limitations. *New Phytologist,* Volume 187, p. 666–681.

Gartner, B. L. et al., 1990. Water Transport Properties of Vine and Tree Stems in a Tropical Deciduous Forest. *American Journal of Botany,* 77(6), pp. 742-749.

Gleason, S. M. et al., 2016. Weak tradeoff between xylem safety and xylem-specific hydraulic efficiency across the world's woody plant species. *New Phytologist,* Volume 209, pp. 123-136.

Hsiao, T. C., 1973. Plant responses to water stress. *Annual Review of Plant Physiology and Plant Molecular Biology,* Volume 24, p. 519–570.

Ingwell, L. L. et al., 2010. The impact of lianas on 10 years of tree growth and mortality on Barro Colorado Island, Panama. *Journal of Ecology,* Volume 98, p. 879–887.

Johnson, D. M. et al., 2013. Contrasting hydraulic strategies in two tropical lianas and their host trees. *American Journal of Botany,* 100(2), p. 374–383.

Katul, G., Manzoni, S., Palmroth, S. & Oren, R., 2010. A stomatal optimization theory to describe the effects of atmospheric CO2 on leaf photosynthesis and transpiration. *Annals of Botany,* Volume 105, p. 431–442.

Kim, Y. et al., 2012. Seasonal carbon dynamics and water fluxes in an Amazon rainforest. *Global Change Biology,* 18(4), pp. 1322-1334.

Lambers, H., Chapin III, F. S. & Pons, T. L., 2008. Chapter 3: Plant Water Relations. In: *Plant Physiological Ecology.* New York: Springer, pp. 163-223.

Laurance, W. F. et al., 2014. Long-term changes in liana abundance and forest dynamics in undisturbed Amazonian forests. *Ecology,* 95(6), p. 1604–1611.

Lockhart, J. A., 1965. An analysis of irreversible plant cell elongation. *Journal of Theoretical Biology,* Volume 8, p. 264–275.

Maréchaux, I. et al., 2017. Stronger seasonal adjustment in leaf turgor loss point in lianas than trees in an Amazonian forest. *Biology Letters,* 13(1).

Maréchaux, I. et al., 2015. Drought tolerance as predicted by leaf water potential at turgor loss point varies strongly across species within an Amazonian forest. *Functional Ecology,* Volume 29, pp. 1268- 1277.

McCulloh, K. A. & Sperry, J. S., 2005. Pattern in hydraulic achitecture and their implications for transport efficiency. *Tree Physiol,* Volume 25, pp. 257-267.

Medlyn, B. E., De Kauwe, M. G. & Duursma, . R. A., 2016. New developments in the effort to model ecosystems under water stress. *New Phytologist,* 212(1), pp. 5-7.

Medvigy, D. et al., 2009. Mechanistic scaling of ecosystem function and dynamics in space and time: Ecosystem Demography model version 2. *Journal of geophysical research,* Volume 114, p. G01002.

Meinzer, F. C., Bond, B. J., Warren, J. M. & Woodruff, D. R., 2005. Does water transport scale universally with tree size?. *Functional Ecology,* Volume 19, p. 558–565.

Meinzer, F. C. et al., 2009. Xylem hydraulic safety margins in woody plants: Coordination of stomatal control of xylem tension with hydraulic capacitance. *Funct Ecol,* Volume 23, p. 922–930.

Moorcroft, P. R., Hurtt, G. C. & Pacala, S. W., 2001. A method for scaling vegetation dynamics: the ecosystem demography model (ED). *Ecological Monographs,* 71(4), p. 557–586.

Pan, Y. et al., 2011. A Large and Persistent Carbon Sink in the World's Forests. *Science,* Volume 333, p. 988–993.

R Core Team, 2017. *R: A language and environment for statistical computing,* Vienna, Austria: R Foundation for Statistical Computing.

Reich, P. B., 2014. The world-wide ‘fast–slow’ plant economics spectrum: a traits manifesto. *Journal of Ecology,* Volume 202, p. 275–301.

Reich, P. B., Walters, M. B. & Ellsworth, D. S., 1997. From tropics to tundra: global convergence in plant functioning. *Proceedings of the National Academy of Sciences (USA),* Volume 94, p. 13730 –13734.

Restom, T. G. & Nepstad, D. C., 2001. Contribution of vines to the evapotranspiration of a secondary forest in eastern Amazonia. *Plant and Soil,* 236(2), p. 155–163.

Rowe, N. & Speck, T., 2005. Plant growth forms: an ecological and evolu- tionary perspective. *New Phytol,* Volume 166, p. 61–72.

Sade, N., Gebremedhin, A. & Moshelion, M., 2012. Risk-taking plants: Anisohydric behavior as a stress-resistance trait. *Plant Signaling & Behavior,* 7(7), p. 767–770.

Santiago, L. & Wright, S. J., 2007. Leaf Functional Traits of Tropical Forest Plants in Telation to Growth Form. *Functional Ecology,* 21(1), pp. 19-27.

Schnitzer, S. A., 2005. A Mechanistic Explanation for Global Patterns of Liana Abundance and Distribution. *The American Naturalist,* 166(2), p. 262–276.

Schnitzer, S. A. & Bongers, F., 2002. The ecology of lianas and their role in forests. *Trends in Ecology & Evolution,* 17(5), pp. 223-230.

Schnitzer, S. A. & Bongers, F., 2011. Increasing liana abundance and biomass in tropical forests: emerging patterns and putative mechanisms. *Ecology Letters,* 14(4), p. 397–406.

Selaya, N. G. et al., 2007. Above-ground Biomass Investments and Light Interception of Tropical Forest Trees and Lianas Early in Succession. *Annals of Botany,* Volume 99, p. 141–151.

Slot, M., Rey-Sanchez, C., Winter, K. & Kitajima, K., 2014. Trait-based scaling of temperature-dependent foliar respiration in a species-rich tropical forest canopy. *Functional Ecology,* 28(5), p. 1074–1086.

Slot, M. & Winter, K., 2017. In situ temperature response of photosynthesis of 42 tree and liana species in the canopy of two Panamanian lowland tropical forests with contrasting rainfall regimes. *New Phytologist,* 214(3), pp. 1103-1117.

Sperry, J. S., Donnelly, J. R. & Tyree, M. T., 1988. A method for measuring hydraulic conductivity and embolism in xylem. *Plant Cell Environ,* Volume 11, p. 35–40.

van der Heijden, G. M. F., Powers, J. S. & Schnitzer, S. A., 2015. Lianas reduce carbon accumulation and storage in tropical forests. *PNAS,* 112(43), p. 13267–13271.

van der Sande, M. T., Poorter, L., Schnitzer, S. A. & Markesteijn, L., 2013. Are lianas more drought-tolerant than trees? A test for the role of hydraulic architecture and other stem and leaf traits. *Oecologia,* Volume 172, pp. 961-972.

Verbeeck, H. & Kearsley, E., 2016. The importance of including lianas in global vegetation models. *PNAS,* 113(1).

Vico, G. et al., 2013. A perspective on optimal leaf stomatal conductance under CO2 and light co-limitations.. *Agricultural and Forest Meteorology,* Volume 182–183, p. 191–199.

Werden, L. K., Waring, B. G., Smith-Martin, C. M. & Powers, J. S., 2017. Tropical dry forest trees and lianas differ in leaf economic spectrum traits but have overlapping water-use strategies. *Tree Physiology,* Volume 38, p. 517–530.

Westoby, M. et al., 2002. Plant ecological strategies: some leading dimensions of variation between species. *Annual Review of Ecology and Systematics,* Volume 33, p. 125–159.

Wright, I. J. et al., 2004. The worldwide leaf economics spectrum. Volume 428, p. 821–827.

Xu, X. et al., 2016. Diversity in plant hydraulic traits explains seasonal and inter-annual variations of vegetation dynamics in seasonally dry tropical forests. *New Phytologist,* Volume 212, p. 80–95.

Yorke, S. R. et al., 2013. Increasing Liana Abundance and Basal Area in a Tropical Forest: The Contribution of Long-distance Clonal Colonization. *Biotropica,* 45(3), p. 317–324.

Zanne, A. et al., 2009. Data from: Towards a worldwide wood economics spectrum. *Dryad Digital Repository.*

Zhu, S.-D. & Cao, K.-F., 2009. Hydraulic Properties and Photosynthetic Rates in Co-occurring Lianas and Trees in a Seasonal Tropical Rainforest in Southwestern China. *Plant Ecology,* 204(2), pp. 295-304.

Zhu, S.-D., Chen, Y.-J., Fu, P.-L. & Cao, K.-F., 2017. Different hydraulic traits of woody plants from tropical forests with contrasting soil water availability. *Tree Physiology,* Volume 37, p. 1469–1477.

8. Appendices

Table S1: Lianas database synthesized from available published an unpublished data $P_{tlp,l}$ $K_{s,sat}$ and $P_{50,x}$

a) Leaf osmotic potential at turgor loss point of liana species

Species name	WD (g/cm^{-3})	SLA (m^2/kg)	$P_{tlp,l}$ (MPa)	Reference	Location
Combretum latifolium	0.460	7.43	-1.29	WD and $P_{tlp,l}$ from Zhu & Cao (2009) SLA from Cai et al. (2009)	Xishuangbanna Tropical Botanical Garden, southern Yunnan, China
Millettia pachycarpa	0.490	9.85	-1.52	WD and $P_{tlp,l}$ from Zhu & Cao (2009) SLA from Cai & Bongers (2007)	Xishuangbanna Tropical Botanical Garden, southern Yunnan, China
Quisqualis indica	0.500		-1.40	Zhu & Cao (2009)	Xishuangbanna Tropical Botanical Garden, southern Yunnan, China
Prionostemma aspera	0.580		-2.07	Johnson et al. (2013)	Parque Natural Metropolitano, Panama
Trichostigma octandrum	0.490		-1.49	Johnson et al. (2013)	Parque Natural Metropolitano, Panama
Schisandra glabra	0.329	22.88	-0.85	$P_{tlp,l}$ from Feild et al. (2009) SLA and WD from Feild & Isnard (2013)	Fagus grandiflora forest near Toccoa, Georgia
Celastrus paniculatus			-1.57	Chen et al. (2017)	Xishuangbanna Tropical Botanical Garden, southern Yunnan, China
Marsdenia sinensis			-1.49	Chen et al. (2017)	Xishuangbanna Tropical Botanical Garden, southern Yunnan, China
Ventilago calyculata			-2.34	Chen et al. (2017)	Xishuangbanna Tropical Botanical Garden, southern Yunnan, China

b) Xylem hydraulic traits of liana species

Species name	WD (g/cm^{-3})	$K_{s,sat}$ ($kg\ m^{-1}\ s^{-1}\ Mpa^{-1}$)	$P_{50,x}$ (MPa)	Reference	Location
Arrabidaea pattellifera	0.410	12.20	-0.26	De Guzman et al. (2016)	Lowland tropical forest in Parque Natural Metropolitano, Panamá
Combretum fruticosum	0.540	5.73	-0.34	De Guzman et al. (2016)	Lowland tropical forest in Parque Natural Metropolitano, Panamá

Doliocarpus dentatus	0.400	5.85	-0.29	De Guzman et al. (2016)	Lowland tropical forest in Parque Natural Metropolitano, Panamá
Hiraea reclinata	0.650	2.91	-0.66	De Guzman et al. (2016)	Lowland tropical forest in Parque Natural Metropolitano, Panamá
Mikania leiostacya	0.220	10.10	-0.33	De Guzman et al. (2016)	Lowland tropical forest in Parque Natural Metropolitano, Panamá
Serjania mexicana	0.330	27.82	-0.22	De Guzman et al. (2016)	Lowland tropical forest in Parque Natural Metropolitano, Panamá
Prionostemma aspera	0.580		-1.14	Johnson et al. (2013)	Parque Natural Metropolitano, Panama
Trichostigma octandrum	0.490		-2.90	Johnson et al. (2013)	Parque Natural Metropolitano, Panama
Fridericia caudigera	0.510		-2.49	$P_{50,x}$ from Carvalho et al. (2016) WD from Carvalho et al. (2015)	Tropical seasonally dry areas in the semiarid region of north-eastern Brazil
Fridericia dispar	0.490		-1.88	$P_{50,x}$ from Carvalho et al. (2016) WD from Carvalho et al. (2015)	Tropical seasonally dry areas in the semiarid region of north-eastern Brazil
Fridericia chica	0.520		-2.09	$P_{50,x}$ from Carvalho et al. (2016) WD from Carvalho et al. (2015)	Tropical seasonally dry areas in the semiarid region of north-eastern Brazil
Schisandra glabra	0.329		-0.80	Feild & Isnard, (2013)	Fagus grandiflora forest near Toccoa, Georgia
Celastrus paniculatus		8.62	-1.42	Chen et al. (2017)	Xishuangbanna Tropical Botanical Garden, southern Yunnan, China
Marsdenia sinensis		10.57	-1.04	Chen et al. (2017)	Xishuangbanna Tropical Botanical Garden, southern Yunnan, China
Ventilago calyculata		4.80	-1.57	Chen et al. (2017)	Xishuangbanna Tropical Botanical Garden, southern Yunnan, China
Millettia pachycarpa	0.510	11.51	-1.10	Zhu et al. (2017)	Tropical Non Karstic Forest in southern Yunnan, China
Uncaria macrophylla	0.410	12.38	-1.00	Zhu et al. (2017)	Tropical Non Karstic Forest in southern Yunnan, China
Byttneria integrifolia	0.370	10.57	-0.90	Zhu et al. (2017)	Tropical Non Karstic Forest in southern Yunnan, China

Combretum latifolium	0.530	4.52	-1.50	Zhu et al. (2017)	Tropical Karstic Forest in southern Yunnan, China
Ventilago calyculata	0.550	5.14	-1.30	Zhu et al. (2017)	Tropical Karstic Forest in southern Yunnan, China
Bauhinia tenuiflora	0.350	92.13	-2.10	Zhu et al. (2017)	Tropical Non Karstic Forest and Karstic Forest in southern Yunnan, China very particular
Bauhinia touranensis	0.330	104.50	-2.20	Zhu et al. (2017)	Tropical Non Karstic Forest and Karstic Forest in southern Yunnan, China very particular
Adenocalymma inundatum	0.570	3.00		Gartner et al. (1990)	Estación de Biología Chamela in the state of Jalisco, Mexico
Aristolochia taliscana	0.230	45.00		Gartner et al. (1990)	Estación de Biología Chamela in the state of Jalisco, Mexico
Combretum fruticosum	0.635	19.00		Gartner et al. (1990)	Estación de Biología Chamela in the state of Jalisco, Mexico
Dieterlea fusiformis	0.270	100.00		Gartner et al. (1990)	Estación de Biología Chamela in the state of Jalisco, Mexico
Entadopsis polystachya	0.420	200.00		Gartner et al. (1990)	Estación de Biología Chamela in the state of Jalisco, Mexico
Gaudichaudia mcvaughii	0.630	21.00		Gartner et al. (1990)	Estación de Biología Chamela in the state of Jalisco, Mexico
Gouania rosei	0.585	110.00		Gartner et al. (1990)	Estación de Biología Chamela in the state of Jalisco, Mexico
Ipomoea bracteata	0.340	30.00		Gartner et al. (1990)	Estación de Biología Chamela in the state of Jalisco, Mexico
Passiflora juliana	0.440	40.00		Gartner et al. (1990)	Estación de Biología Chamela in the state of Jalisco, Mexico
Serjania brachycarpa	0.660	10.00		Gartner et al. (1990)	Estación de Biología Chamela in the state of Jalisco, Mexico

c) Area-based maximum leaf net carbon assimilation rate of lianas species

Species name	**WD (g/cm^{-3})**	**A_{area} ($\mu mol\ m^{-2}\ s^{-1}$)**	**Reference**	**Location**
Combretum fruticosum	0.540	8.60	A_{area} from Avalos et al. (2007) WD from De Guzman et al. (2016)	Parque Natural Metropolitano, near Panama City - Tropical Dry Forest
Cnestidium rufescens	0.770	5.85	Brenes-Arguedas et al. (2013)	Isthmus of Panama
Connarus panamensis	0.700	6.84	Brenes-Arguedas et al. (2013)	Isthmus of Panama
Machaerium	0.680	9.45	Brenes-Arguedas et al.	Isthmus of Panama

microphyllum			(2013)	
Peritassa pruinosa	0.660	4.01	Brenes-Arguedas et al. (2013)	Isthmus of Panama
Ventilago calyculata		4.88	Chen et al. (2014)	Xishuangbanna Tropical Botanical Garden, southern Yunnan, China
Celastrus paniculatus		12.53	Chen et al. (2015)	Xishuangbanna, southern Yunnan, Southwest China
Ventilago calyculata		11.90	Chen et al. (2015)	Xishuangbanna, southern Yunnan, Southwest China
Ventilago calyculata		13.83	Chen et al. (2015)	Xishuangbanna, southern Yunnan, Southwest China
Schisandra glabra	0.329	8.19	A_{area} from Feild et al. (2009) WD from Feild & Isnard (2013)	Fagus grandiflora forest near Toccoa, Georgia
Tasmannia cordata	0.620	4.80	Feild et al. (2012)	Summit trail, Mt Wilhelm, Chimbu Province, Papua New Guinea
Maripa panamensis		12.26	Santiago & Wright (2007)	Lowland tropical forest in Parque Nacional San Loren on the Caribbean coast of Central Panama
Doliocarpus dentatus		10.78	Santiago & Wright (2007)	Lowland tropical forest in Parque Nacional San Loren on the Caribbean coast of Central Panama
Tontelea richardii		7.29	Santiago & Wright (2007)	Lowland tropical forest in Parque Nacional San Loren on the Caribbean coast of Central Panama
Quisqualis indica	0.500	10.50	Zhu & Cao (2009)	Xishuangbanna Tropical Botanical Garden, southern Yunnan, China
Combretum latifolium	0.460	10.85	Zhu & Cao (2009)	Xishuangbanna Tropical Botanical Garden, southern Yunnan, China
Millettia pachycarpa	0.490	12.05	Zhu & Cao (2009)	Xishuangbanna Tropical Botanical Garden, southern Yunnan, China
Combretum fruticosum	0.540	17.70	A_{area} from Slot et al. (2014) WD from De Guzman et al. (2016)	Parque Natural Metropolitano a semideciduous moist tropical forest near Panama City
Mikania leiostachya	0.220	9.80	A_{area} from Slot et al. (2014) WD from De Guzman et al. (2016)	Parque Natural Metropolitano a semideciduous moist tropical forest near Panama City
Serjania mexicana	0.330	12.90	A_{area} from Slot et al. (2014) WD from De Guzman et al. (2016)	Parque Natural Metropolitano a semideciduous moist tropical forest near Panama City
Gouania	0.440	12.70	A_{area} from Slot et al. (2014)	Parque Natural Metropolitano a semideciduous moist tropical forest

lupuloides			WD from Campanello et al. (2016)	near Panama City

Table S2: Tropical forest database reconstructed following Christofferense et al. (2016)

a) Leaf hydraulic traits of tree species

Species name	**WD (g/cm^{-3})**	**$P_{tlp,l}$ (MPa)**	**$P_{0,l}$ (MPa)**
Abarema jupunba	0.585	-1.60	-1.16
Alseis blackiana	0.536	-2.04	-1.14
Anacardium excelsum	0.391	-1.13	-0.93
Anacardium excelsum	0.391	-1.00	-0.81
Apeiba glabra	0.320	-2.02	-1.67
Aspidosperma excelsum	0.792	-1.74	-1.71
Astronium graveolens	0.868	-2.07	-1.15
Balfourodendron riedelianum	0.666	-2.27	-1.86
Barringtonia pendula	0.520	-1.25	-0.80
Bauhinia variegata	0.653	-1.93	-1.54
Bauhinia variegata	0.653	-1.29	-1.22
Bocoa prouacensis	1.054	-2.13	-1.92
Bocoa prouacensis	1.054	-2.23	-1.75
Bocoa prouacensis	1.054	-1.61	-2.01
Bocoa prouacensis	1.054	-1.96	-1.59
Bocoa prouacensis	1.054	-2.08	-1.95
Bocoa prouacensis	1.054	-2.31	-1.60
Bocoa prouacensis	1.054	-2.25	-2.14
Bowdichia virgilioides	0.910	-2.50	-2.09
Brosimum rubescens	0.825	-2.28	-1.98
Bursera simaruba	0.305	-1.39	-1.15
Bursera simaruba	0.305	-0.69	-0.55
Byrsonima sericea	0.780	-2.03	-1.54
Calycophyllum candidissimum	0.697	-1.30	-1.07
Capparis verrucosa	0.860	-3.65	-2.97
Carapa procera	0.564	-1.74	-1.34
Carapa procera	0.564	-2.02	-1.68
Carapa procera	0.564	-1.87	-1.70

Carapa procera	0.564	-1.96	-1.68
Carapa procera	0.564	-2.04	-1.59
Caryocar brasiliense	0.650	-2.20	-1.71
Caryocar glabrum	0.654	-1.88	-1.53
Caryocar glabrum	0.654	-1.28	-1.09
Casearia sylvestris	0.705	-2.73	-2.46
Cassipourea guianensis	0.820	-2.05	-1.49
Cedrela fissilis	0.467	-1.28	-1.00
Celtis philippensis	0.703	-2.62	-2.39
Chrysophyllum sanguinolentum	0.671	-1.45	-0.98
Cleistanthus sumatranus	0.640	-1.72	-1.57
Coffea arabica	0.620	-1.82	-1.48
Conceveiba guianensis	0.543	-1.70	-1.28
Connarus suberosus	0.450	-2.63	-2.25
Cordia alliodora	0.520	-2.16	-1.93
Cordia alliodora	0.520	-1.86	-1.64
Cordia alliodora	0.520	-1.89	-1.71
Cordia alliodora	0.520	-1.97	-1.76
Cordia americana	0.688	-1.58	-1.36
Cordia collococca	0.420	-2.09	-1.80
Cordia dentata	0.500	-2.14	-1.88
Cordia lasiocalyx	0.397	-1.63	-1.48
Cordia sagotii	0.409	-1.95	-1.59
Cordia sagotii	0.409	-1.87	-1.49
Couepia bracteosa	0.770	-2.26	-2.06
Couepia caryophylloides	0.770	-1.87	-1.95
Couratari oblongifolia	0.505	-1.97	-1.61
Couratari oblongifolia	0.505	-1.75	-1.35
Crossopteryx febrifuga	0.702	-1.73	-1.44
Cupania scrobiculata	0.628	-2.13	-1.81
Cupressus torulosa	0.440	-0.81	-0.53
Dicorynia guianensis	0.591	-1.58	-0.99
Dicorynia guianensis	0.591	-1.66	-1.18
Dicorynia guianensis	0.591	-1.51	-2.06
Dicorynia guianensis	0.591	-1.46	-1.80

Dicorynia guianensis	0.591	-2.34	-1.24
Diospyros carbonaria	0.730	-1.81	-1.84
Diospyros carbonaria	0.730	-1.60	-1.42
Drypetes variabilis	0.737	-1.93	-1.56
Drypetes variabilis	0.737	-2.31	-2.02
Enterolobium cyclocarpum	0.390	-1.82	-1.51
Eperua grandiflora	0.704	-1.91	-1.78
Eperua grandiflora	0.704	-2.26	-1.71
Eperua grandiflora	0.704	-1.99	-1.06
Eperua grandiflora	0.704	-2.03	-1.64
Eperua grandiflora	0.704	-1.99	-1.68
Eperua grandiflora	0.704	-2.18	-1.63
Eperua grandiflora	0.704	-2.05	-1.54
Eperua grandiflora	0.704	-2.11	-1.15
Eschweilera coriacea	0.852	-1.66	-1.24
Eschweilera coriacea	0.852	-1.71	-1.68
Eschweilera coriacea	0.852	-1.72	-1.31
Eschweilera coriacea	0.852	-1.98	-1.29
Eschweilera coriacea	0.852	-2.03	-1.72
Eschweilera coriacea	0.852	-1.68	-1.26
Eschweilera coriacea	0.852	-2.01	-1.66
Eschweilera grandiflora	0.876	-1.75	-1.35
Ficus auriculata	0.468	-0.86	NA
Ficus hispida	0.382	-1.23	NA
Ficus insipida	0.377	-2.04	-1.70
Ficus racemosa	0.363	-1.44	NA
Forchhammeria pallida	0.840	-2.83	-2.51
Gliricidia sepium	0.618	-1.60	-1.33
Guettarda acreana	0.870	-1.78	-1.38
Gustavia hexapetala	0.716	-1.96	-1.63
Gustavia hexapetala	0.716	-2.01	-1.66
Gustavia hexapetala	0.716	-1.75	-1.96
Gustavia hexapetala	0.716	-1.92	-1.55
Gustavia hexapetala	0.716	-2.00	-1.35
Gustavia hexapetala	0.716	-2.26	-1.60

Hirtella glandulosa	0.925	-1.89	-1.49
Hybanthus prunifolius	0.670	-1.74	-1.22
Hymenaea courbaril	0.792	-1.44	-1.95
Hymenaea courbaril	0.792	-2.17	-1.81
Hymenaea martiana	0.825	-2.32	-2.03
Hymenosporum flavum	0.607	-2.06	-1.38
Irvingia malayana	0.883	-1.83	-1.69
Iryanthera sagotiana	0.572	-1.83	-1.44
Lecythis persistens	0.860	-1.93	-1.56
Lecythis persistens	0.860	-2.06	-1.71
Lecythis persistens	0.860	-1.74	-1.68
Lecythis persistens	0.860	-2.00	-1.65
Lecythis persistens	0.860	-1.95	-1.58
Lecythis persistens	0.860	-2.03	-1.64
Lecythis persistens	0.860	-1.94	-1.34
Lecythis poiteaui	0.802	-2.20	-1.88
Lecythis poiteaui	0.802	-2.59	-2.35
Lecythis poiteaui	0.802	-2.33	-1.58
Lecythis poiteaui	0.802	-2.64	-2.05
Lecythis poiteaui	0.802	-3.15	-2.42
Licania alba	0.887	-1.90	-1.89
Licania alba	0.887	-1.74	-1.26
Licania alba	0.887	-2.08	-1.68
Licania alba	0.887	-2.03	-1.34
Licania alba	0.887	-2.14	-1.53
Licania alba	0.887	-2.20	-1.91
Licania alba	0.887	-2.22	-1.50
Licania canescens	0.880	-1.95	-1.59
Licania canescens	0.880	-2.12	-1.79
Licania canescens	0.880	-2.07	-1.73
Licania canescens	0.880	-1.70	-1.28
Licania canescens	0.880	-2.33	-1.64
Licania canescens	0.880	-1.99	-1.67
Licania canescens	0.880	-2.20	-1.74
Licania canescens	0.880	-2.02	-1.81

Licania membranacea	0.880	-2.10	-1.61
Licania membranacea	0.880	-2.16	-1.96
Licania membranacea	0.880	-1.97	-1.82
Licania membranacea	0.880	-2.26	-2.60
Licania membranacea	0.880	-2.14	-2.04
Licania membranacea	0.880	-2.79	-1.89
Licania platypus	0.620	-1.41	-1.14
Licaria guianensis	0.748	-2.44	-2.17
Maclura tinctoria	0.795	-1.85	-1.55
Mallotus penangensis	0.590	-1.15	-1.02
Manilkara bidentata	0.873	-3.05	-2.56
Manilkara huberi	0.921	-2.36	-2.08
Manilkara huberi	0.921	-2.13	-1.81
Maytenus obtusifolia	0.750	-3.08	-2.60
Miconia argentea	0.589	-1.81	-1.50
Millettia atropurpurea	0.610	-1.12	-1.01
Minquartia guianensis	0.787	-1.61	-1.18
Morisonia americana	0.880	-4.08	-3.28
Neea floribunda	0.620	-1.91	-1.53
Ochroma pyramidale	0.158	-1.60	-1.37
Ocotea aciphylla	0.511	-1.50	-1.29
Ocotea percurrens	0.519	-1.72	-1.31
Palaquium sumatranum	0.520	-1.88	-1.66
Parashorea densiflora	0.670	-1.83	-1.70
Peltophorum dubium	0.744	-1.36	-1.10
Perebea guianensis	0.560	-1.82	-1.43
Piptocarpha rotundifolia	0.650	-1.75	-1.40
Pourouma tomentosa	0.395	-1.69	-1.27
Pouteria cladantha	0.942	-1.93	-1.56
Pouteria filipes	0.964	-2.20	-1.89
Protium opacum	0.570	-1.90	-1.79
Protium opacum	0.570	-2.12	-1.56
Protium opacum	0.570	-1.93	-1.34
Protium panamense	0.452	-2.66	-2.23
Protium sagotianum	0.558	-2.28	-2.02

Protium sagotianum	0.558	-2.33	-2.48
Protium sagotianum	0.558	-2.31	-1.92
Protium sagotianum	0.558	-2.23	-2.04
Protium trifoliolatum	0.685	-2.34	-1.99
Protium trifoliolatum	0.685	-2.28	-1.98
Pseudobombax septenatum	0.212	-1.28	-0.91
Qualea rosea	0.580	-1.78	-1.38
Quercus oleoides	0.860	-3.12	-2.62
Quercus semiserrata	0.712	-1.42	-1.18
Randia armata	0.668	-1.96	-1.68
Rhododendron arboreum	0.491	-1.74	-1.49
Sapindus saponaria	0.712	-2.14	-1.58
Shorea guiso	0.705	-1.38	-1.21
Shorea macroptera	0.425	-0.93	-0.78
Shorea parvifolia	0.405	-1.10	-0.99
Shorea robusta	0.730	-2.04	-1.58
Tabebuia chrysantha	1.043	-1.49	-0.99
Talisia microphylla	0.817	-2.04	-1.70
Tapirira guianensis	0.457	-2.19	-1.83
Tapura capitulifera	0.721	-1.92	-1.24
Tapura capitulifera	0.721	-1.95	-1.54
Tapura capitulifera	0.721	-1.66	-1.77
Ternstroemia brasiliensis	0.470	-1.88	-1.55
Theobroma subincanum	0.470	-1.66	-1.70
Theobroma subincanum	0.470	-2.04	-3.02
Theobroma subincanum	0.470	-1.74	-1.33
Theobroma subincanum	0.470	-2.11	-1.78
Thouinidium decandrum	0.670	-3.48	-2.30
Trattinnickia aspera	0.424	-2.54	-2.12
Trichilia trifolia	0.800	-1.98	-1.59
Unonopsis rufescens	0.605	-1.52	-1.07
Unonopsis rufescens	0.605	-1.99	-1.69
Unonopsis rufescens	0.605	-1.96	-1.64
Vataireopsis surinamensis	0.570	-1.76	-1.36
Vatica odorata	0.790	-1.27	-1.00

Virola michelii	0.470	-1.84	-1.45
Virola michelii	0.470	-1.64	-1.22
Vochysia ferruginea	0.410	-2.30	-1.92
Vouacapoua americana	0.794	-2.50	-1.53
Vouacapoua americana	0.794	-2.05	-1.70
Vouacapoua americana	0.794	-2.10	-2.25
Vouacapoua americana	0.794	-1.91	-1.86
Vouacapoua americana	0.794	-2.26	-0.98
Vouacapoua americana	0.794	-2.06	-1.77
Xanthophyllum affine	0.613	-1.80	-1.59
Ziziphus mauritiana	0.618	NA	-1.52

b) Xylem hydraulic traits and photosynthetic trait of tree species

Species name	**WD** (g/cm^3)	**$K_{s,sat}$** ($kg\ m^{-1}\ s^{-1}\ Mpa^{-1}$)	**$P_{50,x}$** (MPa)	**A_{area}** ($\mu mol\ m^{-2}\ s^{-1}$)
Acinodendron pohlianum	0.530	4.73	-3.10	NA
Adenocalymma inundatum	0.570	2.50	NA	NA
Agathis ovata	0.559	0.80	-1.77	NA
Aleurites moluccana	0.520	3.57	-2.17	11.79
Alphitonia excelsa	0.670	4.89	-5.56	7.19
Amborella trichopoda	NA	NA	-3.00	NA
Amyxa pluricornis	0.630	NA	-0.63	NA
Anacardium excelsum	0.390	NA	-1.56	NA
Annona glabra	0.510	9.10	-3.30	NA
Annona glabra	0.120	NA	NA	NA
Araucaria columnaris	NA	NA	-3.30	NA
Araucaria hunsteinii	0.568	NA	-4.07	NA
Araucaria laubenfelsii	0.800	0.27	-2.40	NA
Ardisia palmana	NA	0.23	NA	NA
Aristolochia taliscana	0.230	45.00	NA	NA
Aspidosperma desmanthum	0.700	NA	NA	9.70
Aspidosperma tomentosum	0.600	1.56	NA	NA
Aspidosperma tomentosum	0.545	4.02	NA	NA
Aspidosperma tomentosum	0.497	3.55	NA	NA
Austrobaileya scandens	NA	2.30	NA	4.29
Bischofia javanica	0.430	6.16	-1.27	14.35

Blepharocalyx salicifolius	0.550	21.00	-1.40	NA
Blepharocalyx salicifolius	0.330	4.73	-2.17	NA
Blepharocalyx salicifolius	0.310	5.37	-2.30	NA
Blepharocalyx salicifolius	0.560	NA	NA	NA
Blepharocalyx salicifolius	0.530	2.05	-1.93	NA
Blepharocalyx salicifolius	0.490	2.28	-1.72	NA
Bourreria cumanensis	NA	0.41	-3.82	NA
Brachychiton australis	0.250	6.46	-3.17	8.85
Bursera simaruba	0.305	NA	-0.90	NA
Bursera simaruba	0.305	NA	-1.00	NA
Bursera simaruba	0.305	3.55	NA	NA
Byrsonima crassa	0.520	49.00	-0.90	NA
Byrsonima crassa	0.530	NA	NA	NA
Byrsonima crassifolia	0.584	2.10	NA	NA
Caesalpinia eriostachys	0.700	1.70	NA	NA
Calycophyllum candidissimum	0.697	NA	-2.87	NA
Calycophyllum candidissimum	0.697	1.11	NA	NA
Capparis aristiguetae	NA	0.11	-2.45	NA
Capparis indica	0.560	0.90	NA	NA
Carapa guianensis	0.530	NA	-0.80	NA
Caryocar brasiliense	0.350	3.50	-2.03	NA
Caryocar brasiliense	0.590	NA	NA	NA
Caryocar brasiliense	0.380	3.88	-1.97	NA
Caryocar brasiliense	0.350	2.67	-1.48	NA
Caryocar brasiliense	0.340	2.78	-1.62	NA
Cassipourea guianensis	0.820	1.30	-4.80	NA
Cassipourea guianensis	0.820	NA	-4.68	NA
Ceanothus greggii	0.606	0.63	-6.00	NA
Chrysophyllum cainito	0.655	NA	-2.10	NA
Chrysophyllum cainito	0.610	NA	NA	9.90
Clusia stenophylla	NA	0.12	NA	NA
Clusia uvitana	NA	1.07	-1.30	NA
Cnidoscolus spinosus	0.310	3.00	NA	NA
Cochlospermum gillivraei	0.300	7.75	-1.44	7.02
Codiaeum variegatum	0.490	0.86	-2.23	7.22

Comarostaphylis polifolia	0.650	0.67	-4.00	11.67
Combretum fruticosum	0.635	18.00	NA	NA
Cordia alba	NA	1.50	-3.60	NA
Cordia alliodora	0.520	NA	-3.20	NA
Cordia alliodora	0.520	NA	-3.20	NA
Cordia alliodora	0.520	9.56	-3.60	NA
Cordia alliodora	0.520	11.00	-2.93	NA
Cordia alliodora	0.520	NA	-3.00	NA
Cordia alliodora	0.520	8.93	-1.78	NA
Cordia alliodora	0.470	NA	NA	15.40
Cordia alliodora	0.590	2.90	NA	NA
Cordia cymosa	NA	7.81	-1.20	NA
Cordia inermis	NA	1.84	NA	NA
Cordia lasiocalyx	0.397	3.76	-2.57	NA
Cordia lucidula	NA	3.32	-1.58	NA
Cordia macrocephala	NA	2.27	NA	NA
Cordia nodosa	0.390	3.72	-2.34	NA
Cordia panamensis	NA	11.63	-2.33	NA
Cosmibuena valerioi	NA	0.39	NA	NA
Coursetia ferruginea	NA	1.26	-2.42	NA
Curatella americana	0.390	NA	-1.48	NA
Curatella americana	0.650	1.25	NA	NA
Dalbergia miscolobium	0.636	NA	NA	9.80
Dalbergia miscolobium	0.530	NA	NA	NA
Dalbergia miscolobium	0.670	NA	NA	NA
Dendropanax latilobus	NA	0.64	NA	NA
Dieterlea fusiformis	0.270	90.00	NA	NA
Diospyros dictyoneura	NA	NA	-0.42	NA
Diospyros mindanaensis	0.650	NA	-0.79	NA
Dipterocarpus globosus	0.700	NA	-0.18	NA
Drimys granadensis	0.455	NA	-1.64	NA
Drimys granadensis	NA	0.39	NA	NA
Drimys insipida	0.554	NA	-4.68	NA
Dryobalanops sumatrensis	0.650	NA	-0.26	NA
Drypetes indica	0.670	0.60	-2.32	4.29

Dussia munda	0.530	NA	NA	12.30
Entada polystachya	0.420	210.00	NA	NA
Enterolobium cyclocarpum	0.390	NA	-2.73	NA
Enterolobium cyclocarpum	0.390	3.50	NA	NA
Eriotheca pubescens	0.600	2.67	NA	NA
Eriotheca pubescens	0.540	4.33	NA	NA
Eriotheca pubescens	0.497	4.21	NA	NA
Erythroxylum suberosum	0.633	0.41	NA	NA
Eucalyptus miniata	0.898	3.13	NA	NA
Eucalyptus tetrodonta	0.922	2.50	-6.27	NA
Eupomatia laurina	0.544	NA	-0.40	NA
Eupomatia laurina	0.544	1.12	NA	NA
Ficus citrifolia	0.400	NA	-1.60	NA
Ficus citrifolia	0.400	NA	-1.60	NA
Ficus insipida	0.290	NA	-1.66	NA
Ficus insipida	0.377	NA	-1.90	NA
Ficus insipida	0.340	NA	NA	19.20
Galbulimima belgraveana	0.501	NA	-1.30	NA
Garrya ovata	0.744	2.75	-6.60	7.32
Gaudichaudia mcvaughii	0.630	20.00	NA	NA
Gliricidia sepium	0.618	3.65	NA	NA
Gnetum	NA	1.80	NA	8.00
Gnetum costatum	NA	1.12	-3.10	13.23
Gnetum gnemon	0.610	1.10	-4.62	13.45
Gnetum latifolium	NA	1.65	NA	8.98
Gonocaryum	NA	4.60	NA	NA
Gossia bidwillii	0.710	1.24	-5.12	4.17
Gouania rosei	0.585	110.00	NA	NA
Guapira	0.475	1.70	NA	NA
Guapira areolata	0.460	8.10	NA	NA
Guapira noxia	0.498	2.56	NA	NA
Guapira noxia	0.496	3.70	NA	NA
Guapira noxia	0.497	4.80	NA	NA
Guarea guidonia	0.467	7.70	NA	NA
Guatteria dumetorum	0.420	NA	NA	12.20

Hedyosmum goudotianum	NA	NA	-1.74	NA
Hedyosmum mexicanum	NA	NA	-0.79	NA
Heliocarpus pallidus	0.470	5.50	NA	NA
Heritiera sumatrana	0.530	NA	-1.69	NA
Hevea brasiliensis	0.467	NA	-2.69	NA
Hevea brasiliensis	0.467	0.18	-1.50	NA
Hevea brasiliensis	0.467	3.60	-1.42	NA
Hevea brasiliensis	0.467	NA	-2.72	NA
Hevea brasiliensis	0.467	0.18	-2.04	NA
Hevea brasiliensis	0.467	3.60	-1.22	NA
Hevea brasiliensis	0.480	4.38	-1.27	14.18
Hibiscus	NA	9.20	NA	27.90
Homalanthus novoguineensis	NA	3.87	NA	26.00
Horsfieldia	NA	1.45	NA	NA
Humiriastrum diguense	0.580	NA	NA	11.20
Hybanthus prunifolius	0.670	NA	-2.60	NA
Hymenaea courbaril	0.792	NA	-3.00	NA
Hymenaea courbaril	0.792	2.40	NA	NA
Hymenaea martiana	0.560	2.94	-2.80	NA
Hymenaea stigonocarpa	0.720	3.59	-3.17	NA
Idiospermum australiense	0.650	NA	-0.62	NA
Ipomoea bracteata	0.340	35.00	NA	NA
Ipomoea wolcottiana	0.605	2.20	NA	NA
Juniperus barbadensis var. Lucayana	0.399	4.84	-6.30	NA
Juniperus barbadensis var. Lucayana	0.625	0.71	-8.30	NA
Kielmeyera coriacea	0.660	32.00	-0.80	NA
Kielmeyera coriacea	0.500	NA	NA	NA
Kielmeyera coriacea	NA	NA	-1.91	NA
Kielmeyera coriacea	0.455	0.93	NA	11.50
Kleinhovia hospita	0.429	8.20	NA	NA
Laguncularia racemosa	0.610	2.38	-3.40	NA
Lonchocarpus dipteroneurus	NA	0.98	-1.77	NA
Lophopetalum subobovatum	0.540	NA	-0.59	NA
Luehea seemannii	0.330	NA	NA	17.00
Macaranga denticulata	0.410	4.41	-1.14	16.72

Mallotus wrayi	NA	NA	-0.53	NA
Manilkara bidentata	0.873	NA	-2.70	NA
Manilkara bidentata	0.610	NA	NA	10.30
Manilkara chicle	1.040	0.45	NA	NA
Marila laxiflora	0.480	NA	NA	9.90
Miconia	NA	0.51	NA	NA
Miconia cuspidata	0.740	5.37	-3.40	NA
Miconia minutiflora	0.500	NA	NA	16.80
Morisonia americana	0.880	0.14	-2.39	NA
Myrsine coriacea	0.620	3.25	-3.08	NA
Myrsine guianensis	0.520	2.00	-2.12	NA
Nectandra purpurascens	0.550	NA	NA	11.10
Ochroma pyramidale	0.190	2.10	-1.00	NA
Ocotea insularis	0.580	NA	NA	12.60
Oreopanax nubigenus	NA	0.48	NA	NA
Ouratea hexasperma	0.410	1.69	-2.03	NA
Ouratea hexasperma	0.420	1.62	-1.87	NA
Ouratea hexasperma	0.420	1.11	-1.48	NA
Ouratea hexasperma	0.460	0.96	-1.48	9.70
Ouratea lucens	NA	NA	-1.80	NA
Ouratea lucens	NA	NA	-1.80	NA
Passiflora juliana	0.440	40.00	NA	NA
Payena endertii	0.633	NA	-0.63	NA
Pentace adenophora	NA	NA	-0.19	NA
Pereskia marcanoi	0.700	2.06	NA	NA
Pereskia portulacifolia	0.600	2.69	NA	NA
Pinus caribaea	0.364	14.68	-1.91	NA
Pinus caribaea	0.450	4.70	-3.27	NA
Piper aduncum	NA	7.82	NA	NA
Piper betle	NA	1.06	NA	NA
Pithecellobium dulce	0.684	0.54	-1.65	NA
Podocarpus neriifolius	0.477	0.45	NA	NA
Poulsenia armata	0.430	NA	NA	11.80
Pourouma bicolor	0.450	NA	NA	13.70
Prioria copaifera	0.414	NA	-1.60	NA

Protium	0.440	7.40	NA	NA
Protium panamense	0.452	NA	-1.70	NA
Pseudobombax septenatum	0.250	1.60	-1.00	NA
Psidium sartorianum	0.725	1.10	NA	NA
Psychotria horizontalis	NA	NA	-4.90	NA
Psychotria horizontalis	NA	NA	-4.90	NA
Qualea grandiflora	0.606	0.99	NA	NA
Qualea grandiflora	0.520	2.22	NA	NA
Qualea grandiflora	0.570	2.05	NA	11.90
Qualea grandiflora	NA	NA	NA	11.90
Qualea parviflora	0.460	1.26	-2.23	NA
Qualea parviflora	0.450	1.70	-2.50	NA
Qualea parviflora	0.569	NA	NA	NA
Qualea parviflora	0.480	0.94	-1.65	10.40
Qualea parviflora	0.480	1.15	-1.72	NA
Qualea parviflora	0.280	47.00	-1.00	NA
Quercus oleoides	0.860	NA	-3.03	NA
Quercus oleoides	0.860	2.10	NA	NA
Quercus sebifera	0.710	0.71	-5.50	9.81
Rehdera trinervis	NA	NA	-2.80	NA
Rehdera trinervis	NA	1.72	NA	NA
Rhipidocladum racemiflorum	NA	10.20	-4.50	NA
Rhizophora mangle	0.898	0.40	-6.30	NA
Rhizophora mangle	0.898	1.40	-4.40	NA
Rhus standleyi	0.577	2.49	-2.70	7.96
Ruprechtia fusca	0.625	2.40	NA	NA
Salvia candicans	0.689	0.73	-7.30	23.75
Santiria mollis	NA	NA	-0.20	NA
Schefflera macrocarpa	0.460	3.23	-2.17	NA
Schefflera macrocarpa	0.560	2.67	-2.43	NA
Schefflera macrocarpa	0.540	NA	NA	NA
Schefflera macrocarpa	0.590	0.96	-1.77	NA
Schefflera macrocarpa	0.560	2.14	-1.72	16.30
Schefflera morototoni	0.280	NA	-1.68	NA
Schefflera morototoni	0.456	NA	-1.38	NA

Schefflera pittieri	NA	0.65	NA	NA
Sclerolobium paniculatum	0.620	NA	NA	13.70
Sclerolobium paniculatum	0.650	4.20	-3.40	16.20
Sclerolobium paniculatum	0.670	3.60	-3.20	14.20
Sclerolobium paniculatum	0.590	6.00	-3.40	14.80
Sclerolobium paniculatum	0.580	NA	-3.60	18.70
Serjania brachycarpa	0.660	10.00	NA	NA
Shorea faguetiana	0.480	NA	-0.37	NA
Shorea mecistopteryx	0.427	NA	-0.63	NA
Shorea ovalis	0.430	NA	-0.39	NA
Simarouba amara	0.410	NA	NA	17.50
Simarouba amara	0.383	NA	-2.00	NA
Simarouba amara	0.383	1.20	NA	NA
Spondias purpurea	0.390	2.90	NA	NA
Styrax ferrugineus	NA	NA	-3.35	NA
Styrax ferrugineus	0.490	2.59	-3.35	NA
Styrax pohlii	0.540	3.45	-2.00	NA
Swartzia simplex	NA	NA	-2.90	NA
Swietenia macrophylla	0.520	NA	-2.20	NA
Swietenia macrophylla	0.520	1.20	NA	NA
Symplocos lanceolata	0.380	1.62	-1.50	NA
Symplocos mosenii	0.480	4.78	-1.60	NA
Tachigali versicolor	0.521	NA	-1.60	NA
Tapirira guianensis	0.457	NA	-1.80	NA
Tapirira guianensis	0.430	NA	NA	12.90
Tinospora	NA	10.15	NA	NA
Trattinnickia aspera	0.424	NA	-1.10	NA
Trattinnickia aspera	0.570	NA	NA	12.20
Trema orientalis	0.345	5.87	NA	NA
Trichospermum pleiostigma	NA	7.67	NA	NA
Trimenia neocaledonica	NA	NA	-1.25	NA
Virola sebifera	0.500	NA	NA	13.50
Vochysia ferruginea	0.410	NA	-1.00	NA
Vochysia ferruginea	0.350	NA	NA	18.30
Vochysia thyrsoidea	0.420	NA	NA	NA

Zygogynum baillonii	NA	NA	-3.00	NA
Zygogynum bicolor	NA	NA	-2.30	NA
Zygogynum crassifolium	0.659	NA	-4.54	NA
Zygogynum pancheri	0.628	NA	-5.20	NA
Zygogynum pomiferum	0.575	NA	-3.45	NA
Zygogynum queenslandianum	NA	NA	-3.60	NA
Zygogynum semecarpoides	0.408	NA	-3.27	NA
Aspidosperma cruenta	NA	1.56	NA	NA
Anacardium excelsum	0.391	NA	NA	NA
Cecropia longipes	NA	NA	NA	NA
Cordia alliodora	NA	NA	NA	NA
Luehea seemannii	0.417	8.76	NA	NA
Schefflera morototoni	0.456	NA	NA	NA
Spondias mombin	0.391	NA	NA	NA
Amphipterygium adstringens	0.480	5.36	-0.96	NA
Apoplanesia paniculata	0.560	0.99	-4.61	NA
Bursera heteresthes	0.400	10.24	-1.36	NA
Bursera instabilis	0.400	15.40	-2.54	NA
Caesalpinia eriostachys	0.850	4.95	-2.07	NA
Caesalpinia sclerocarpa	0.710	2.60	-2.51	NA
Cochlospermum vitifolium	0.270	NA	NA	NA
Cordia alliodora	0.630	1.21	-3.18	NA
Cordia elaeagnoides	0.540	1.59	-1.15	NA
Esenbeckia nesiotica	1.060	0.43	-4.74	NA
Gliricidia sepium	0.640	14.82	-0.85	NA
Heliocarpus pallidus	0.550	9.67	-0.66	NA
Haematoxylon brasiletto	0.810	NA	NA	NA
Piptadenia constricta	0.730	1.53	-1.94	NA
Plumera rubra	0.350	NA	NA	NA

c) Xylem water potential at full turgor of tree species

Species name	**WD (g/cm^3)**	**$P_{0,x}$ (MPa)**
Holocalyx balansae	0.858	-0.76
Parapiptadenia rigida	0.757	-0.67
Lonchocarpus muehlbergianus	0.698	-0.76

Balfourodendron riedelianum	0.659	-1.50
Chrysophyllum gonocarpum	0.595	-1.16
Cordia trichotoma	0.508	-1.98
Cabralea canjerana	0.528	-0.90
Ocotea diospyrifolia	0.541	-1.64
Cedrela fissilis	0.492	-0.53
Ceiba speciosa	0.308	-0.51
Schefflera morototoni	0.280	-0.76
Anacardium excelsum	0.390	-1.17
Ficus insipida	0.400	-1.40
Cordia alliodora	0.520	-2.51
Manilkara bidentata	0.665	-2.21
Tapirira guianensis	0.520	-1.45
Trattinnickia aspera	0.540	-0.83
Schefflera macrocarpa	0.539	-1.34
Blepharocalyx salicifolius	0.559	-1.35
Qualea parviflora	0.570	-1.30
Caryocar brasiliense	0.590	-1.26
Schefflera morototoni	0.456	-0.77
Ochroma pyramidale	0.190	-0.69
Pseudobombax septenatum	0.250	-0.98
Spondias purpurea	0.330	-1.43
Albizia guachapele	0.513	-1.97
Calycophyllum candidissimum	0.697	-2.62
Simarouba glauca	0.465	-1.83

Table S3: Additional data of tree species used for t-test of area-based maximum leaf net carbon assimilation rate from Xu et al. (2016)

Species name	**WD (g/cm^3)**	**A_{area} (µmol m^{-2} s^{-1})**
Didymopanax macrocarpum	0.760	10.00
Andira inermis	0.635	9.50
Licania arborea	0.650	8.00
Pithecellobium saman	0.480	10.50
Psidium guajava	0.800	6.30

Jacquinia pungens	0.810	13.00
Aspidosperma tomentosum	0.820	10.20
Bowdichia virgilioides	0.910	9.20
Caryocar brasiliense	0.650	9.40
Connarus suberosus	0.450	12.20
Piptocarpha rotundifolia	0.650	12.30
Castanopsis chinensis	0.540	11.74
Castanopsis fissa	0.500	10.11
Diospyros morrisiana	0.480	7.85
Melicope pteleifolia	0.430	11.17
Sapium sebiferum	0.570	12.95
Schefflera heptaphylla	0.590	13.00
Schima superba	0.470	9.31
Toxicodendron succedaneum	0.510	11.58
Acmena acuminatissima	0.600	7.77
Acronychia pedunculata	0.540	6.58
Aida canthioides	0.790	6.46
Aporusa dioica	0.570	4.31
Ardisia quinquegona	0.520	7.79
Blastus cochinchinensis	0.510	6.00
Cryptocarya chinensis	0.520	8.02
Cryptocarya concinna	0.500	6.19
Diplospora dubia	0.860	4.08
Gironniera subaequalis	0.640	6.69
Machilus chinensis	0.500	6.71
Memecylon ligustrifolium	0.480	7.06
Microdesmis caseariifolia	0.550	4.93
Mischocarpus pentapetalus	0.720	7.18
Psychotria rubra	0.730	7.51
Pygeum topengii	0.770	5.12
Sarcosperma laurinum	0.620	6.55
Syzygium levinei	0.530	3.83
Syzygium rehderianum	0.630	5.78
Xanthophyllum hainanense	0.590	5.91
Brosimum utile	0.520	6.72

Chrysophyllum cainito	0.780	6.86
Cojoba rufescens	0.740	7.29
Hymenaea courbaril	0.680	5.19
Inga marginata	0.520	10.31
Inga multijuga	0.510	6.59
Lacmellea panamensis	0.520	5.86
Licania hypoleuca	0.710	5.50
Ormosia macrocalyx	0.500	8.41
Pouteria reticulate	0.610	4.51
Pterocarpus rohrii	0.470	3.56
Tocoyena pittieri	0.610	4.34
Manilkara bidentata	0.680	4.22
Oxandra panamensis	0.450	3.86
Plumeria rubra	0.300	8.42
Thevetia ovata	0.670	9.14
Bursera fagaroides	0.450	8.74
Bursera instabilis	0.530	10.24
Caesalpina coriaria	0.840	11.13
Caesalpina platyloba	0.850	6.89
Ceiba grandiflora	0.460	10.87
Ceiba aesculifolia	0.550	13.24
Coccoloba liebmannii	0.600	8.87
Coccoloba barbadensis	0.560	10.00
Cordia alliodora	0.590	15.83
Cordia dentata	0.510	6.29
Jatropha bullockii	0.310	11.81
Jatropha chamelensis	0.310	10.68
Gliricidia sepium	0.650	14.52
Enterolobium cyclocarpum	0.620	7.16
Lonchocarpus magallanesii	0.810	6.46
Lonchocarpus constrictus	0.780	5.90
Tabebuia crysantha	0.700	7.47
Tabebuia rosea	0.450	9.94
Ficus racemosa	0.361	16.40
Ficus scobina	0.275	12.30

Mallotus nesophilus	0.311	13.20
Melaleuca leucadendra	0.336	18.70
Terminalia microcarpa	0.424	13.30
Wrightia pubescens	0.268	9.60
Brachychiton megaphyllus	0.323	10.60
Buchanania obovata	0.450	10.60
Erythrophleum chlorostachys	0.477	10.90
Eucalyptus tetrodonta	0.476	11.10
Planchonia careya	0.360	10.60
Syzygium suborbiculare	0.378	11.10
Terminalia ferdinandiana	0.397	9.40
Cochlospermum fraseri	0.387	9.40
Corymbia foelscheana	0.541	12.90
Melaleuca viridiflora	0.417	14.10
Planchonia careya	0.411	10.20
Syzygium eucalyptoides ssp. Bleeseri	0.301	8.30
Terminalia ferdinandiana	0.439	12.90
Xanthostemon paradoxus	0.387	11.70
Acacia auriculiformis	0.415	14.40
Lophostemon lactifluus	0.421	8.40
Melaleuca viridiflora	0.466	14.10
Aspidosperma cruenta	0.700	9.70
Dussia munda	0.530	12.30
Guatteria dumentorum	0.420	12.20
Humiriastrum diguense	0.580	11.20
Manilkara bidentata	0.610	10.30
Marila laxiflora	0.480	9.90
Miconia borealis	0.500	16.80
Nectandra purpurascens	0.550	11.10
Ocotea ira	0.580	12.60
Poulsenia armata	0.430	11.80
Pourouma bicolor	0.450	13.70
Simarouba amara	0.410	17.50
Tapirira guianensis	0.430	12.90
Trattinickia aspera	0.570	12.20

Virola sebifera	0.500	13.50
Vochysia ferruginea	0.350	18.30
Chrysophyllum cainito	0.610	9.90
Cordia alliodora	0.470	15.40
Ficus insipida	0.340	19.20
Luehea seemannii	0.330	17.00
Hevea brasiliensis	0.480	14.18
Macaranga denticulata	0.410	16.72
Bischofia javanica	0.430	14.35
Drypetes indica	0.670	4.29
Aleurites moluccana	0.520	11.79
Codiaeum variegatum	0.490	7.22
Anisoptera costata	0.549	13.70
Dipterocarpus alatus	0.621	20.30
Dipterocarpus intricatus	0.568	14.70
Dipterocarpus retusus	0.478	14.00
Dipterocarpus tuberculatus	0.401	18.90
Dipterocarpus turbinatus	0.609	16.10
Hopea chinensis	0.621	9.90
Hopea hainanensis	0.533	10.10
Hopea hongayensis	0.655	6.10
Hopea mollissima	0.602	7.20
Parashorea chinensis	0.512	8.30
Shorea assamica	0.342	10.70
Shorea robusta	0.436	17.20
Shorea spp.	0.566	9.70
Vatica guangxiensis	0.578	5.10
Vatica mangachapoi	0.573	9.30
Vatica xishuangbannaensis	0.585	7.30
Cleistanthus sumatranus	0.690	10.00
Lasiococca comberi	0.670	10.10
Celtis philippensis	0.620	10.20
Turpinia pomifera	0.540	9.90
Alphonsea mollis	0.580	9.10
Pistacia weinmannifolia	0.690	13.30

Bauhinia variegata	0.460	9.10
Lagerstroemia tomentosa	0.660	8.20
Croton yanhuii	0.610	12.90
Cipadessa baccifera	0.550	14.70
Millettia cubittii	0.520	8.70
Ficus pisocarpa	0.530	16.20